STUDY OF DRAG REDUCTION BY USING GUAR GUM AND GUM ARABIC MIXTURES

ABDUL RAZZAK KABBARA

FACULTY OF ENGINEERING
UNIVERSITY OF MALAYA
KUALA LUMPUR

2021

STUDY OF DRAG REDUCTION BY USING GUAR GUM AND GUM ARABIC MIXTURES

ABDUL RAZZAK KABBARA

RESEARCH PROJECT SUBMITTED IN PARTIAL FULFILMENT OF THE REQUIREMENTS FOR THE DEGREE OF MASTER OF MECHANICAL ENGINEERING

FACULTY OF ENGINEERING
UNIVERSITY OF MALAYA
KUALA LUMPUR

2021

UNIVERSITY OF MALAYA
ORIGINAL LITERARY WORK DECLARATION

Name of Candidate: Abdul Razzak Kabbara

Matric No: 17222375

Name of Degree: Master of Mechanical Engineering

Title of Project Paper/Research Report/Dissertation/Thesis (“this Work”):

Study of Drag Reduction by using Guar Gum and Gum Arabic Mixtures

Field of Study: Drag Reduction

I do solemnly and sincerely declare that:

(1) I am the sole author/writer of this Work;
(2) This Work is original;
(3) Any use of any work in which copyright exists was done by way of fair dealing and for permitted purposes and any excerpt or extract from, or reference to or reproduction of any copyright work has been disclosed expressly and sufficiently and the title of the Work and its authorship have been acknowledged in this Work;
(4) I do not have any actual knowledge nor do I ought reasonably to know that the making of this work constitutes an infringement of any copyright work;
(5) I hereby assign all and every rights in the copyright to this Work to the University of Malaya (“UM”), who henceforth shall be owner of the copyright in this Work and that any reproduction or use in any form or by any means whatsoever is prohibited without the written consent of UM having been first had and obtained;
(6) I am fully aware that if in the course of making this Work I have infringed any copyright whether intentionally or otherwise, I may be subject to legal action or any other action as may be determined by UM.

Candidate’s Signature Date: 30-July-2021

Subscribed and solemnly declared before,

Witness’s Signature Date:

Name:

Designation

ABSTRACT

Since Toms documented drag reduction in 1949, many researched all over the world are exploring different drag reducing agents hoping to better understand the drag reduction phenomenon and hoping to find best agents for different applications. Many drag reducing agents offered great drag reduction but due to their negative effects on the environment, the focus is switching to biopolymers, a natural ecofriendly alternative. So far, few studies explored the potential of biopolymers to reduce drag, and fewer number of studies tested biopolymer mixers. In this research, guar gum and gum Arabic mixtures of three different ratios at 300 ppm concentration were examined using a closed loop piping system. To study drag reduction as well as the mixture's resistance to heat, two tests were performed for each mixture both at bulk temperature of 30°C. One test without any heating while the other involved continuous heat flux of 3400 W. Several interesting conclusions were found. First, as the ratio of guar gum increased in the mixture, the drag reduction increased. The best drag reduction of 22.65% was achieved by the mixture composed of 50% Guar Gum with 50% Gum Arabic. Finally, for all the fluids considered in the study and for velocities greater than 1 m/s, heating reduced drag reduction.

Keywords: Drag Reduction, Biopolymer, Guar Gum, Gum Arabic

ACKNOWLEDGEMENT

First, I would like express my sinceree sense of gratitude to my wife, Imane, for her boundless love, inspiration, support, patience and understanding throughout my studies. To my son, you have no idea how much energy and motivation you have given me every day. Also, I deeply thank my parents, my brothers and sister for their continuous support and encouragements.

I sincerely thank my supervisor Prof. Kazi Salim Newaz for his continuous guidance, support, encouragement and patience. It was an amazing experience to carry out this research under your supervision.

Special thanks goes to Prof. Farazila Binti Yusof for her unique support at different occasions during my studies.

Also, I would to thank Dr. Afrin Jahan, Siew Boon Keat, Dr. Bhinitha Chandra, Suga Ganeshan A /L Kalaichalvan, Dr. Mohd Nashrul Bin Mohd Zubir, Dr. L. Harish kumar, Mohamed Moustafa Abdelhalim Ahmed Eid, Mr. Zaman, Dr. Waqar Ahmed and Chin Chong Ho for their great help and support during my work at the lab.

Finally, thank you GOD for the countless blessings you have given me.

TABLE OF CONTENTS

LIST OF FIGURES

LIST OF TABLES

LIST OF SYMBOLS AND ABBREVIATIONS

DRA : Drag Reduction Agent

GA : Gum Arabic

GG : Guar Gum

hr : Hour

L : Liter

LPM : Liters per Minute

m^2 : Squared Meter

m^3 : Cubic Meter

MFS : Master Fluid Sample

PAA : Poly acrylic acid

PAAM : Polyacrylamide

PEO : Poly ethylene oxide

PNVF : Poly N-vinyl formamide

Re : Reynolds Number

RPM : Revolutions per Minute

SS : Stainless Steel

VFD : Variable Frequency Drive

CHAPTER 1: INTRODUCTION

1.1 Background and Motivation

It is amazing how adding traces of material as little as 10 parts per million concentrations into a flowing fluid can significantly reduce the pumping energy consumption. This phenomenon is called drag reduction (DR) and it was discovered about 7 decades ago. Since then, many studies tested the drag reduction of different material like polymers and surfactants. Numerous drag reducing material were recognized for their excellent abilities to reduce drag and as a result found their way into many applications. For example, they are used in oil transportation (Al-Sarkhi, 2010), firefighting, irrigation, transport of suspensions and slurries, cooling and heating systems, airplane tank filling and sewage systems (Tamano, Ikarashi, Morinishi, & Taga, 2015). Three decades ago, natural polymers, also called biopolymers, got the attention of research because they offer an environmentally friendly DR solution and also due to the fact that other drag reducing agents (DRA) from petroleum source are finite (Hasan & Abdel-Raouf, 2018). Despite that many studies were carried out to understand the DR phenomenon as it has significant potential to reduce the energy demand of pumping systems that account for a big share of the global energy demand, it still has no model that explains all the facts (Asidin, Suali, Jusnukin, & Lahin, 2019; Brostow, 2008; L. C. Edomwonyi-Otu, A. I. Dosumu, & N. Yusuf, 2021).

1.2 Problem Statement

Transportation of fluids for different purposes is influenced by the pumping power consumption and researchers have been searching and validating different means to reduce the related pumping costs. Drag reducing additives, when added into fluids in appropriate concentrations, may significantly reduce the energy losses and therefore the costs. Present research has been carried out to explore novel natural, ecofriendly additive mixtures for application in drag reduction.

1.3 Objectives

There are two (2) objectives of this project:

- To validate the drag reduction capabilities of novel mixtures of guar gum and gum Arabic at different mixing ratios.
- To determine whether heating has an effect on the drag reduction performance of the mixture.

1.4 Thesis Outline

Chapter 1 introduces an overview of the background of this area and presents the motivation and objectives of this research project.

Chapter 2 includes a literature review on methods, mechanism, theories, methods, experiments, and correlations related to drag reduction with a focus on biopolymers as drag reducing agents.

Chapter 3 Provides a thorough description of the test rig used in this study. Also, it discusses in detail the procedures followed with respect to material preparation, experimental works and data collection.

Chapter 4 Presents and critically discusses the results of this study. Pressure drop, friction factor and drag reduction are plotted versus velocity for the five (5) different fluids that are considered in this study.

Chapter 5 includes a summary of this project highlighting the key outcomes. It also offers few recommendations for related future works.

CHAPTER 2: LITERATURE REVIEW

2.1 Introduction

This chapter presents the available theories, application, and methods of drag reduction with a focus on the recent studies on natural polymers as drag reducing agents.

2.2 Drag Reduction

2.2.1 Mechanism and Applications

Drag reduction in fluid flow is the reduction of frictional forces between the fluid being transported and the solid wall surface to decrease the pumping power consumption (Gharehkhani et al., 2017; Yu et al., 2020). Despite that many researches were carried out to understand this phenomenon as it has significant potential to reduce the energy demand of pumping systems that account for a big share of the global energy demand, and also although that it was discovered 70 years ago, it still has no model that explains all the facts (Asidin et al., 2019; Brostow, 2008; L. C. Edomwonyi-Otu et al., 2021).

So far, the dominant theory about the mechanism of polymer induced drag reduction (PIDR) is the theory of polymer elongation, also called the viscous theory which ponders DRA's as shock absorbers (Asidin et al., 2019; Soares et al., 2019). Lumley (1969) argued that drag reduction is a result of suppression of the energy dissipated by turbulent eddies near the conduit wall. Referring to Figure 2.1, the laminar sublayer will move to the buffer region and begins to vibrate. It will then accelerate near the turbulent core where it becomes unstable and bursts. Due to fluctuating shear in the buffer layer, when DRA is added, it causes an increase in the extensional viscosity as the coiled polymers are stretched. The higher viscosity induced by the DRA dampen the turbulent bursts and as a result minimizing energy wastes and pressure losses due to friction (Asidin et al., 2019; Bin Hasan & Khalid, 2017).

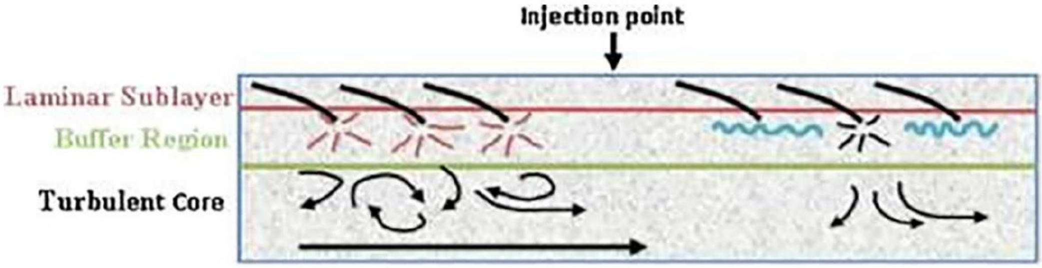

Figure 2.1: Illustration of the Main Theory of Drag Reduction

Drag reducing agents have been used in many applications, including Oil pipelines (Al-Sarkhi, 2010), firefighting, Irrigation, transport of suspensions and slurries, water heating and cooling systems, airplane tank filling, sewage systems. Some countries, like India, actually use DR in their sewer systems in When the existing sewer systems cannot meet the demand of expanding population, (Brostow, 2008). Japan, for example widely use DRA's in cooling and heating systems (Tamano et al., 2015).

2.2.2 Methods

There are two means to reduce drag; additives and non-additives methods (Asidin et al., 2019). As a reaction to uplift the safety and environmental impacts of synthetic additives, many researchers focused on non-additives drag reduction method. Another advantage of this method is that it does not alter the properties of the fluid that they are added into. The method mainly revolves around modifying the wall surface of the conduits or injection of microbubbles. It may be further broken down into passive type utilizing for example riblets, dimples and compliant surfaces or active type that uses oscillating walls (Abdulbari, Yunus, Abdurahman, & Charles, 2013; Asidin et al., 2019). In the other method of drag reduction, which is the additives method, drag reducing agents (DRA's) are added into the fluid being transported. DRA's may be polymers, surfactants or suspended solids (Abdulbari et al., 2013).

Solid suspensions are insoluble DRA's that have two types: fibrous and non-fibrous suspensions and both of these types are found from natural sources (Asidin et al., 2019). Surfactants have high drag reduction potential and they can be classified as anionic, cationic, and non-ionic (Gong, Shen, Dai, Li, & Gong, 2021). Their main advantage is that they have self-repairing characteristic that makes them resistant to mechanical degradation however being toxic and difficult to biodegrade limit their usage. The third type of DRA's is polymers. To reduce drag they can be premixed with the solvent or directly injected into the flow (See Figure 2.2). They are grouped into two types: synthetic and natural (Tiong, Kumar, & Saptoro, 2015). Many researchers studied synthetic polymers. Their drawbacks include vulnerability to chemical and mechanical degradation. They are also resistant to biodegradation, so they have an environmental problem. Main water-soluble types include Poly ethylene oxide (PEO), Polyacrylamide (PAAM), Poly acrylic acid (PAA) and Poly N-vinyl formamide (PNVF). Biopolymers are currently under research focus for their ability to reduce drag without compromising the environment. They are discussed in the next sections.

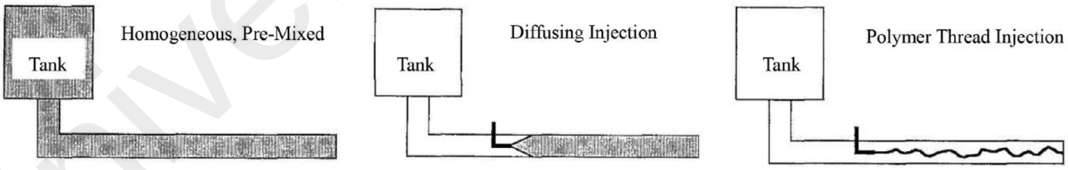

Figure 2.2: Different Methods of adding Polymers in Flows (Manzhai, Nasibullina, Kuchevskaya, & Filimoshkin, 2014)

2.3 Biopolymers

This section presents an overview over the origins, chemical structure, composition, processing and applications of some of the main biopolymers used as DRA's.

2.3.1 Guar Gum

Guar gum (GG) is a natural non-ionic, water soluble polysaccharide extracted from the refined endosperm of cluster bean seeds. It has other names like Guaran, Cyamopsis gum, Guarina, Glucotard and Guyan (George, Shah, & Shrivastav, 2019; Hasan & Abdel-Raouf, 2018).

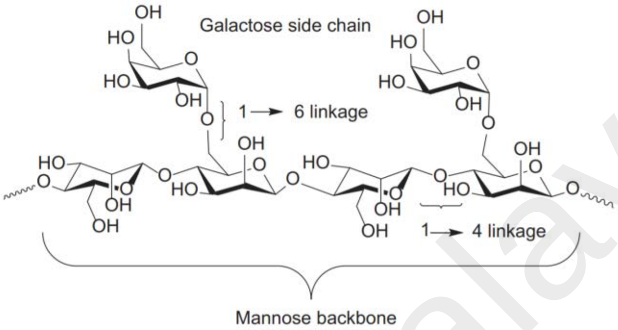

Figure 2.3 Chemical Structure of Guar Gum (D. Verma & Sharma, 2021)

GG is made up of 5.0% protein, 2.0% acidic insoluble ash, 0.7% fat, 80% galactomannan, 12% water. Chemically it is composed of linear polymeric chains of (1-4)-β-D-mannopyranosyl elements having α-D-galactopyranosyl components connected by 1–6 linkages. Its chemical structure is shown in Figure 2.3 (D. Verma & Sharma, 2021).

As shown in Figure 2.4, it has numerous applications in different industries. For example, it is used in corrosion protection, drilling fluids and also to improve viscosity. It is used in our food, our medicines and in cosmetics. For example, it is used in making bread, ice cream, shaving creams, toothpastes, lipsticks and many medications (Saya et al., 2021).

Figure 2.4: Different applications of guar gum (Sharma et al., 2018)

It is extracted through several stages of roasting, grinding, sieving, and polishing as shown in Figure 2.5 (D. Verma & Sharma, 2021).

Figure 2.5: Flow chart showing the extraction process of guar gum (George et al., 2019)

2.3.2 Gum Arabic

Gum Arabic, also known as gum acacia, Arabic gum, acacia, gum sudani, Senegal gum and Indian gum, is a water-soluble biopolymer used in many industries like cosmetics, ceramics, textile, printing, pottery and pharmaceutical (Khalid et al., 2021; Sokhal, Dasaroju, & Bulasara, 2019; C. Verma & Quraishi, 2021). Also, it is also widely used in food industries. For example it is in beverages, chewing gums, shampoos and bath gels (Johnson, 2005). Gum arabic (GA) is basically a blend of polysaccharides and glycoproteins that are both biodegradable (Oprea & Oprea, 2013). It is composed of 1, 3-linked β–d-galactopyranosyl units with two to five 1,3-linked β-d-galactopyranosyl units, joined to the main chain by 1,6-linkages (See Figure 2.6).

Gum arabic is produced from the Acacia tree. As shown in Figure 2.7, it bleeds through cracks in the outer layer of the tree. The exudate quickly dries, then collected, graded and sold as hard drops. (Johnson, 2005).

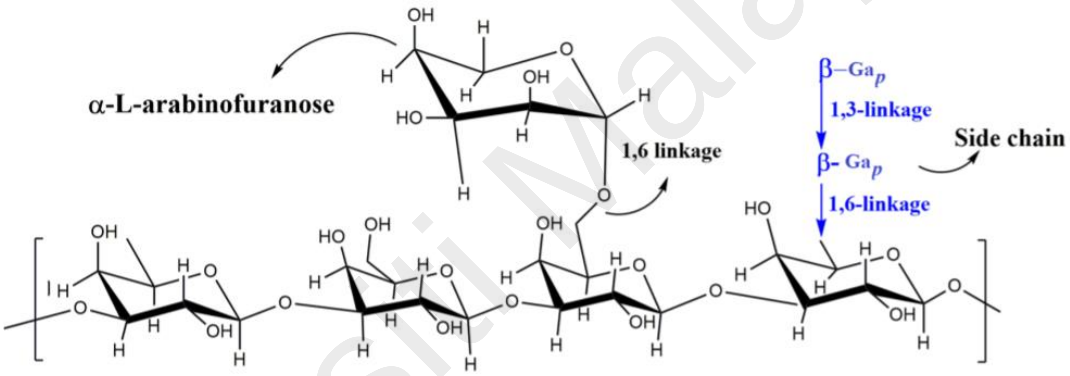

Figure 2.6: Chemical structure of Gum acacia (Mate & Mishra, 2020)

Figure 2.7: Gum arabic exuding from Senegal tree

2.3.3 Xanthan gum

Xanthan gum is the first natural biopolymer produced at an industrial scale (Habibi & Khosravi-Darani, 2017). It was discovered more than 7 decades ago by the United Sates Department of Agriculture (USDA) (Kumar, Rao, & Han, 2018). In 1969, it was approved by the United States Food and Drug Administration (FDA). Xanthan gum is a microbial exo-polysaccharide produced by Xanthomonas bacteria. Its molecular structure is shown in Figure 2.8. It has some excellent properties. For example, it has high molecular weight, easily soluble in water, and it offers high viscosity at minute concentrations. XG is non-toxic, non-sensitizing, and does not cause any irritations for the eye or skin.

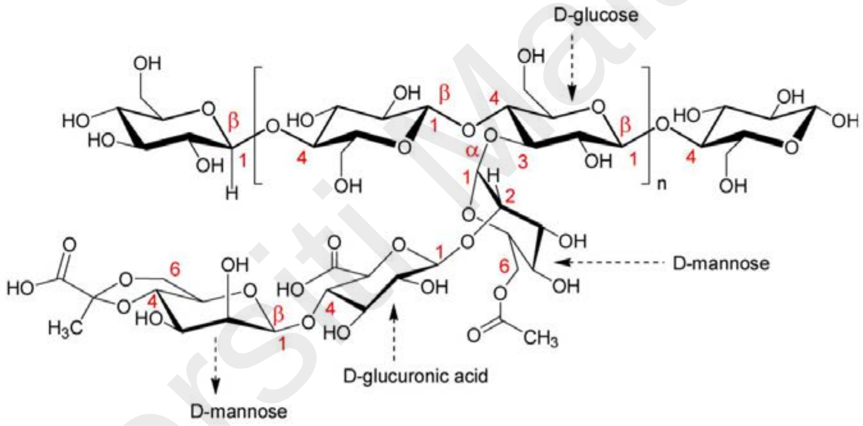

Figure 2.8: Chemical Composition of XG (Maji & Maiti, 2021)

Today, XG exists in many different applications as shown in Table 2.1. For example, it is used in food packaging, water-treatment, toiletries, drugs, cosmetics, water-based paints, construction materials, oil & gas industry and expected to be used in tissue engineering (Kumar et al., 2018).

Table 2.1: Applications of XG (Palaniraj & Jayaraman, 2011)

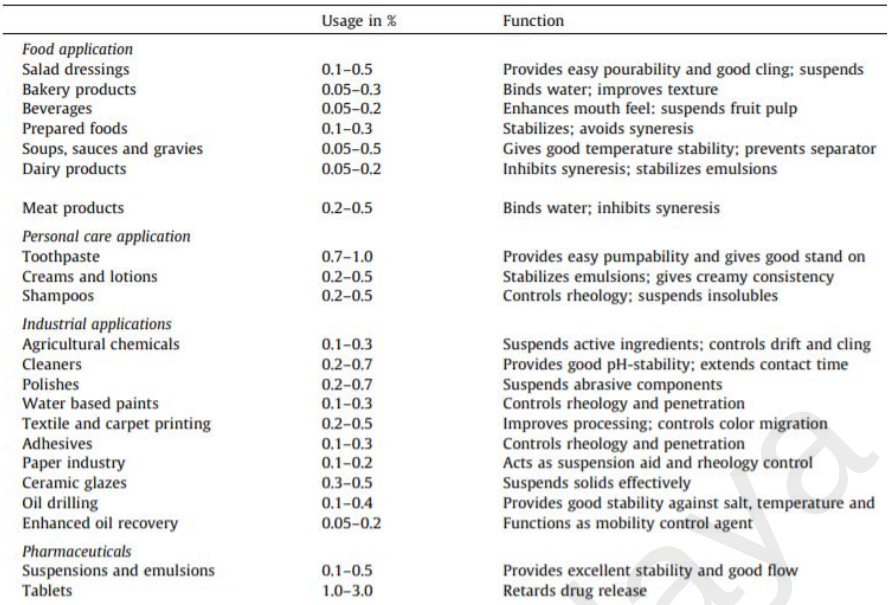

	Usage in %	Function
Food application		
Salad dressings	0.1–0.5	Provides easy pourability and good cling; suspends
Bakery products	0.05–0.3	Binds water; improves texture
Beverages	0.05–0.2	Enhances mouth feel: suspends fruit pulp
Prepared foods	0.1–0.3	Stabilizes; avoids syneresis
Soups, sauces and gravies	0.05–0.5	Gives good temperature stability; prevents separator
Dairy products	0.05–0.2	Inhibits syneresis; stabilizes emulsions
Meat products	0.2–0.5	Binds water; inhibits syneresis
Personal care application		
Toothpaste	0.7–1.0	Provides easy pumpability and gives good stand on
Creams and lotions	0.2–0.5	Stabilizes emulsions; gives creamy consistency
Shampoos	0.2–0.5	Controls rheology; suspends insolubles
Industrial applications		
Agricultural chemicals	0.1–0.3	Suspends active ingredients; controls drift and cling
Cleaners	0.2–0.7	Provides good pH-stability; extends contact time
Polishes	0.2–0.7	Suspends abrasive components
Water based paints	0.1–0.3	Controls rheology and penetration
Textile and carpet printing	0.2–0.5	Improves processing; controls color migration
Adhesives	0.1–0.3	Controls rheology and penetration
Paper industry	0.1–0.2	Acts as suspension aid and rheology control
Ceramic glazes	0.3–0.5	Suspends solids effectively
Oil drilling	0.1–0.4	Provides good stability against salt, temperature and
Enhanced oil recovery	0.05–0.2	Functions as mobility control agent
Pharmaceuticals		
Suspensions and emulsions	0.1–0.5	Provides excellent stability and good flow
Tablets	1.0–3.0	Retards drug release

Xanthan gum is produced by fermentation using the gram-negative bacterium Xanthomonas campestris (Palaniraj & Jayaraman, 2011). Figure 2.9 below illustrate the main manufacturing steps of XG.

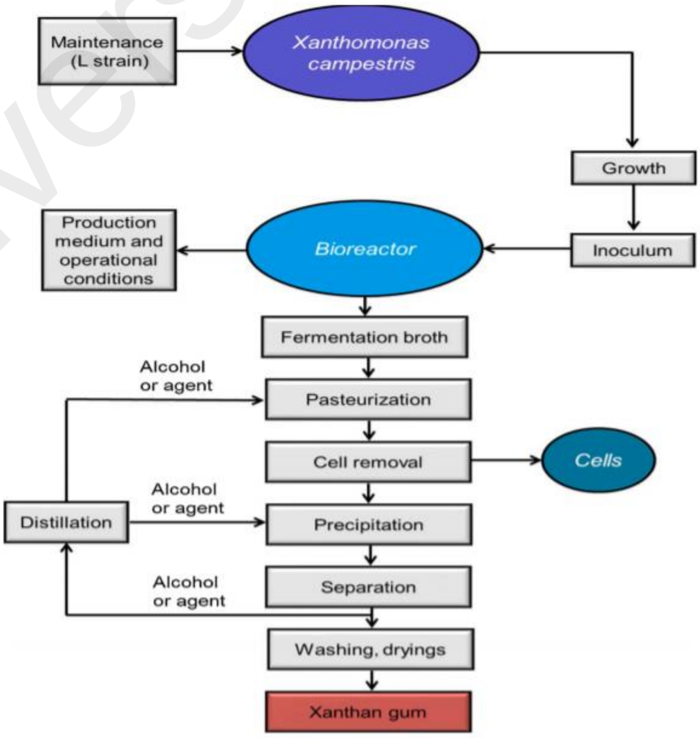

Figure 2.9: Process of XG production (Abu Elella et al., 2021)

2.4 Analysis Studies

Drag reduction analysis includes Reynolds number, pressure loss friction factor and drag reduction ratio. The related equations are presented and discussed in the following subsections.

2.4.1 Reynolds Number

The Reynolds number (Re) is defined as the ratio of inertial forces to viscous forces (Yu et al., 2020). It separates the flow into three types as per Table 2.2 and illustrated in Figure 2.10 (Çengel, 2015).

Table 2.2: Reynolds Numbers for Different Flow Types

Reynolds Number	Type of Flow
$Re < 2300$	Laminar
$2300 \leq Re \leq 4000$	Transitional
$Re > 4000$	Turbulent

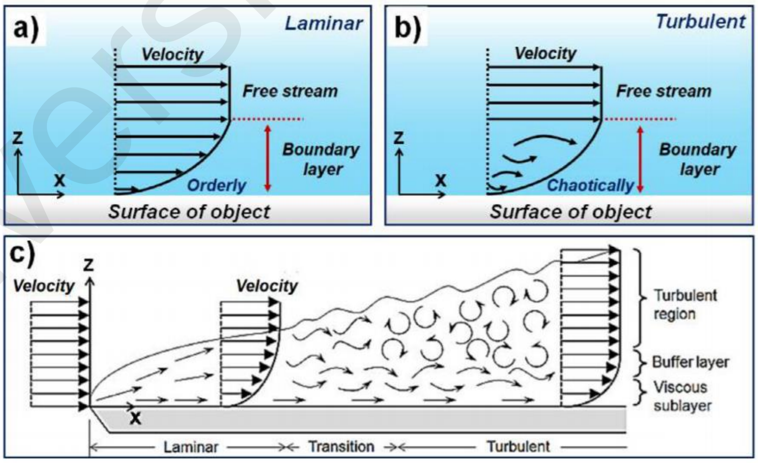

Figure 2.10: Fluid Flow Types in Boundary Layer (Yu et al., 2020)

For circular pipes, it can be expressed as follow:

$$Re = \frac{\rho v D}{\mu} \tag{2.1}$$

Where ρ is the density of the fluid, v is the velocity of the fluid, D is the internal diameter of the pipe and μ is the kinematic viscosity of the fluid.

2.4.2 Drag Reduction Percentage

The Drag Reduction Percentage (%DR) is calculated using the experimental pressure data from the following equation (Al-Sarkhi, 2010; L. C. Edomwonyi-Otu et al., 2021)

$$\%DR = \frac{\Delta P_{Fluid} - \Delta P_{DRA}}{\Delta P_{Fluid}} \text{ x } 100 \tag{2.2}$$

Where ΔP Fluid is the pressure drop without additives while ΔPDRA is the pressure drop with DRA.

2.4.3 Fluid Velocity

Flow rate is calculated from the flow rate (Q) reading collected during the experiment and the wetted cross-sectional area of the pipe using the below equation:

$$V = \frac{Q}{A} \tag{2.3}$$

2.4.4 Pressure Drop

Pressure drop is calculated from the pressure readings taken during the experiment using the flowing equation:

$$PD = \frac{\Delta P}{L} \tag{2.4}$$

Where ΔP is the pressure difference and L is the length of the test section

2.4.5 Friction Factor

The experimental friction factor is calculated using Darcy–Weisbach equation:

$$\Delta P = f \frac{L}{D} \frac{\rho v^2}{2} \tag{2.5}$$

The following standard empirical correlations are used to validate the test rig results:

Colebrook equation:

$$\frac{1}{\sqrt{f}} = -2.0\, log \left(\frac{\varepsilon/D}{3.7} + \frac{2.51}{Re\sqrt{f}} \right) \tag{2.6}$$

Haaland equation:

$$\frac{1}{\sqrt{f}} = -1.8\, log \left[\frac{6.9}{Re} + \left(\frac{\varepsilon/D}{3.7} \right)^{1.11} \right] \tag{2.7}$$

First Petukhov equation:

$$f \;=\; (0.790 \ln Re - 1.64)^{\,-2} \tag{2.8}$$

Blasius equation:

$$f \;=\; 0.3164\, Re^{\,-1/4} \tag{2.9}$$

2.5 Drag Reduction Experiments

2.5.1 Guar Gum

Dosumu, Edomwonyi-Otu, Yusuf, and Abubakar (2020) studied the application of guar gum as a flow enhancer in water as well as oil-water flows. They used a closed loop experimental setup (as shown in Figure 2.11) with 12- and 20-mm piping. First, a master solution of 10000 ppm was prepared and left to hydrate for 12 hours. Then the solution was diluted to prepare 50 to 500 ppm concentrations.

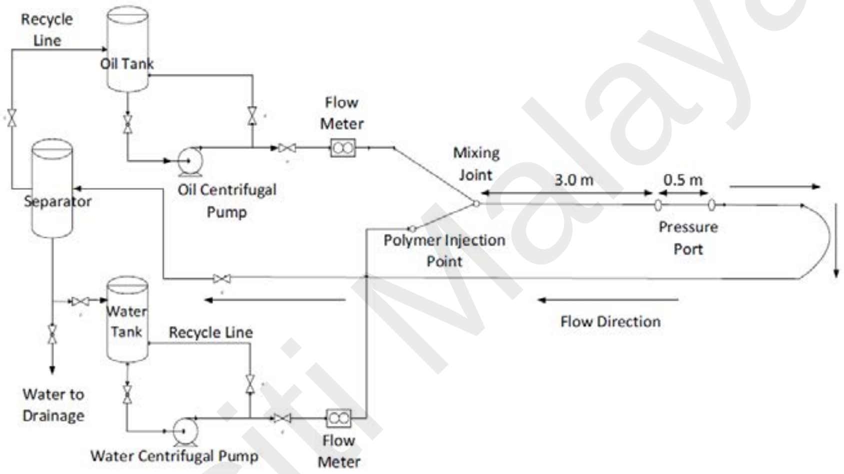

Figure 2.11: Schematic of the test rig used by Dosumu et al. (2020)

Their experiment basically composed of two parts. The first involving only water at different Re numbers and with GG concentration ranging from 50 – 250 ppm. The best drag reduction achieved was 45% at 150-250 ppm and Re 69500 (see Figure 2.12).

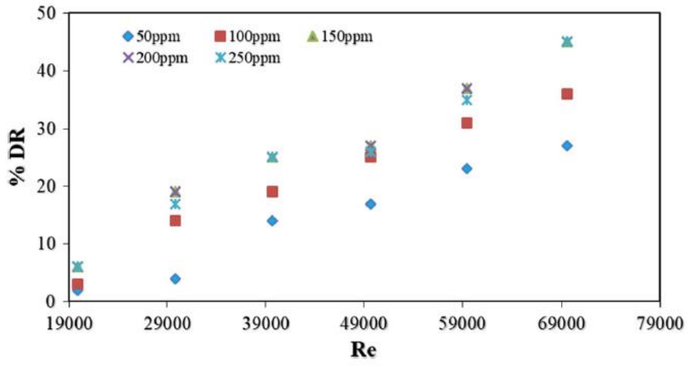

Figure 2.12: %DR versus Re for different concentration in 12 mm ID pipe

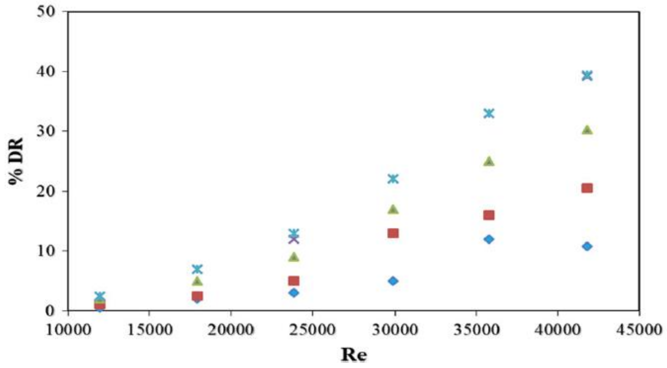

Figure 2.13: %DR versus Re for different concentration in 20 mm ID pipe

The second part of their experiment involved oil-water mixtures at differnet oil fraction at different flow velocities with only 200 ppm GG. They concluded that the higher the oil fraction the lowere the DR.

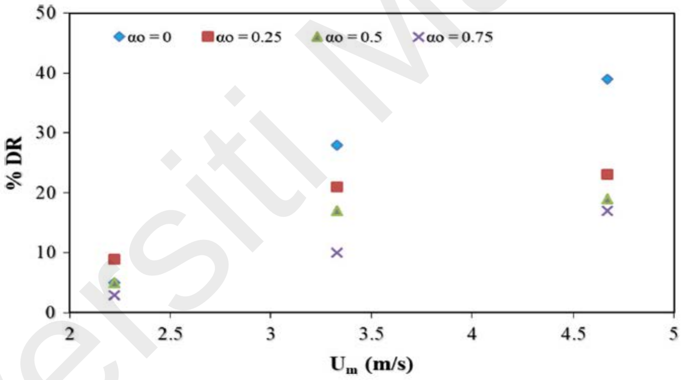

Figure 2.14: %DR versus velocity using 200 ppm DRP for different oil fractions in 12 mm ID pipe

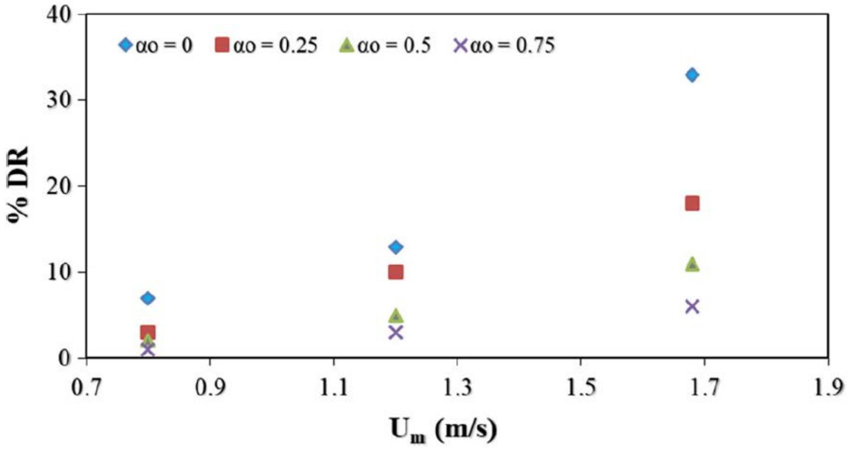

Figure 2.15: %DR versus velocity using 200 ppm DRP for different oil fractions in 12 mm ID pipe

Using a similar setup, L. Edomwonyi-Otu, A. Dosumu, and N. Yusuf (2021) also studied the addition of 200 ppm GG in oil-water flows. They got a DR of about 45% at Re 70000 in fresh water flow. With respect to oil, for flow speeds of 3.33 and 4.67 m/s, DR experienced a significant decrease of about 20% as the fraction of oil introduced increased. While for lower speed of 2.22 m/s, the DR was more or less stable.

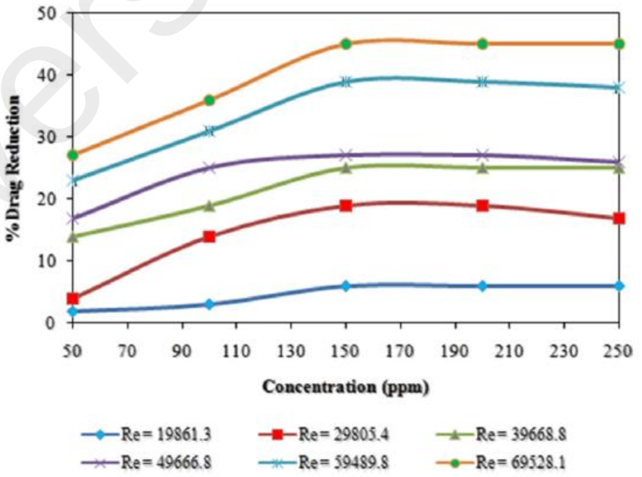

Figure 2.16: GG DR versus concentration using 1.2 cm ID pine

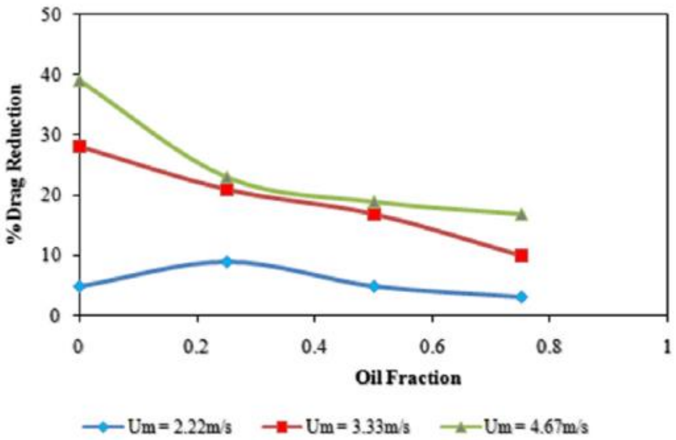

Figure 2.17: Figure 2.18: GG DR versus oil fraction for different velocities using 1.2 cm ID pine

2.5.2 Gum Arabic

Sokhal et al. (2019) studied the effect of injection of the water-soluble gum Arabic near the boundary layer on drag reduction. Their test rig was mainly a galvanized iron, 19.05 mm inner diameter closed loop. It included a tank, centrifugal pump, pressure sensor, rotameter and a peristaltic pump to control the injection rate of the master sample. The master sample was prepared as 10000 ppm and diluted as necessary during the experiment. It was mixed for 7 hours and left overnight to hydrate. The length of the test section was 3045 mm. The gum Arabic used in the experiment was 100 mesh size powder. Tap water was used throughout the experiment and it was maintained at 25 deg. C.

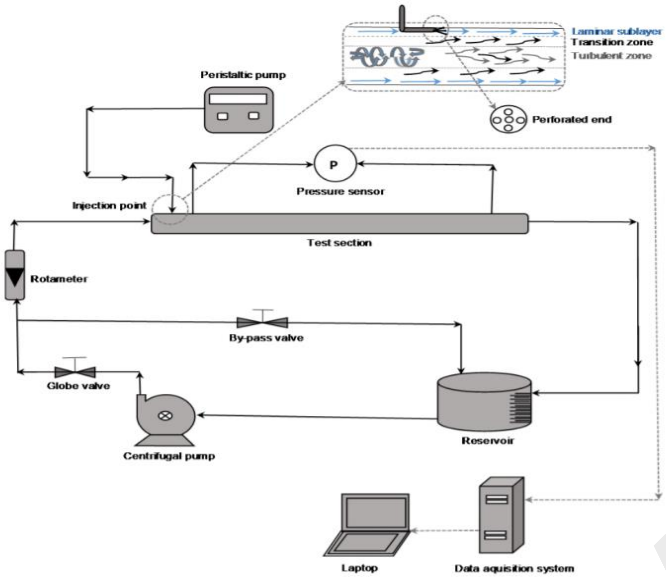

Figure 2.19: Schematic of the test rig used by Sokhal et al. (2019)

The first part of their experiment is to study the effect of adding gum Arabic by injection. While, in the second part, once the required concertation reached, they stopped injection, kept the solution circulating at Re 45000 and continued to monitor the data for 1400 cycles to study the effect of shear, generated by the centrifugal pump, on the polymer effectiveness or also called shear degradation.

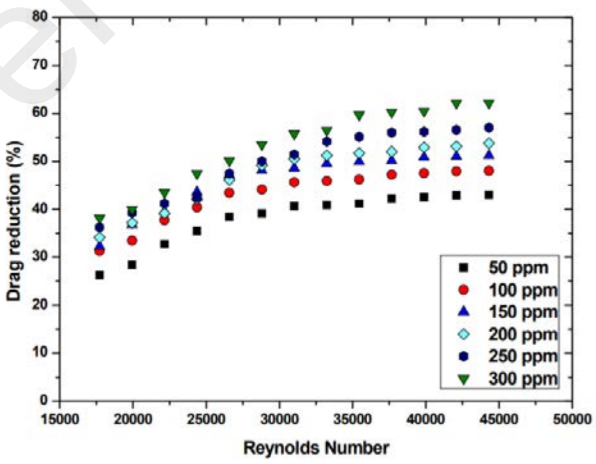

Figure 2.20: DR versus Re number

Sokhal et al. (2019) concluded that the maser sample concentration and Re number have significant effect on drag reduction. The best result of 62.1% drag reduction was found at the highest Re used 45000 and highest concentration 300 ppm. They also observed a continuous decrease in the drag reduction with time. On average a 35% drop in drag reduction for low concentrations (up to 150 ppm) and a 45% drop for concentrations equal for greater than 200 ppm. Finally, their third important conclusion they made is that the injection of the polymer solution in the boundary layer yields better results than premixed solutions.

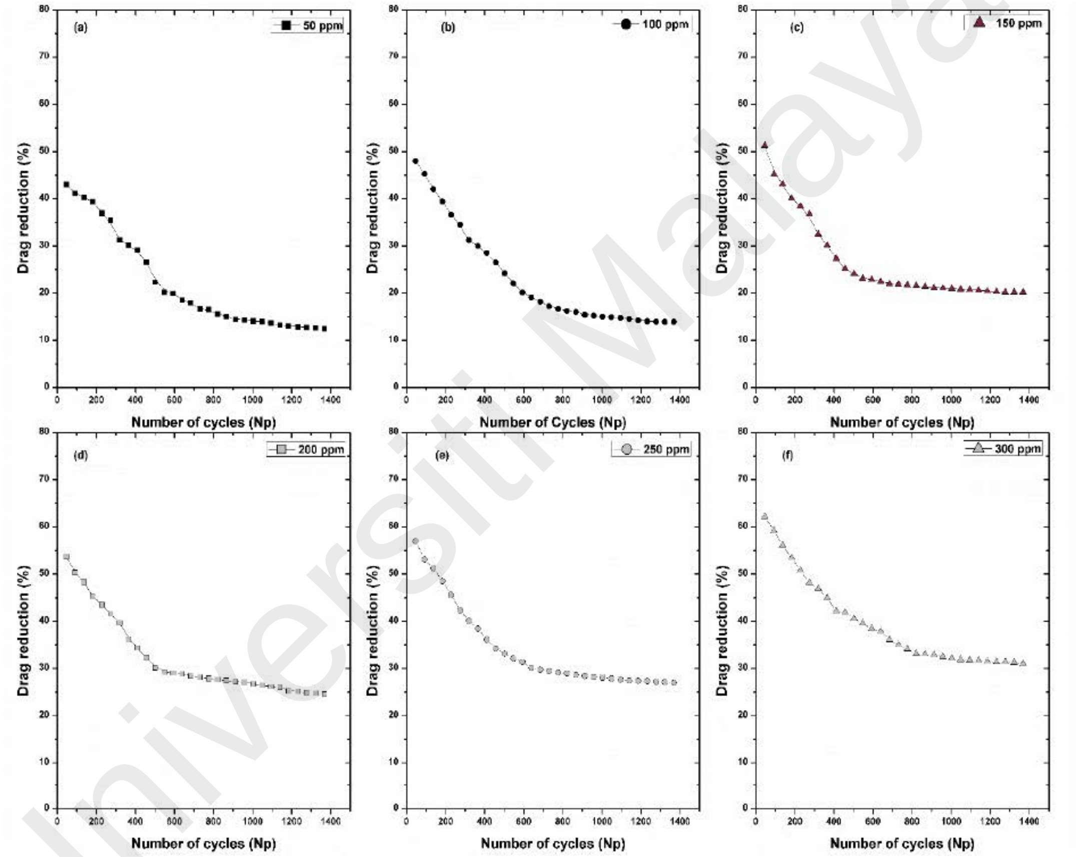

Figure 2.21: Effect of shear degradation on DR for different concentrations

2.5.3 Xanthan Gum

Zhang, Zhou, and Kang (2020) tested xanthan gum (XG) in circular and corrugated pipes. The concentration range they used is from 200 to 3500 ppm. All their tests were used with water as the solvent. In line with the literature, they left the concentrations for

24 hrs to ensure that the molecules are fully dissolved before commencing with the experiment.

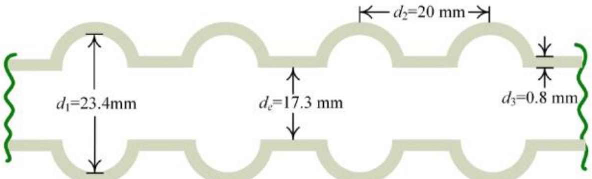

Figure 2.22: Diagram of the corrugate tube used by Zhang et al. (2020)

The results they found were quite interesting. In circular pipes, and in low velocities, DR drops down as concentration increases. While at higher velocities, DR increases until it hits a plateau. XG in corrugated tubes experience a totally different behavior. Except for concentration above 2000 ppm, DR decreases as the bulk velocity of the flow increase. For concentration 2000 and 3500 ppm, the DR rapidly increase then decrease with increasing flow velocity.

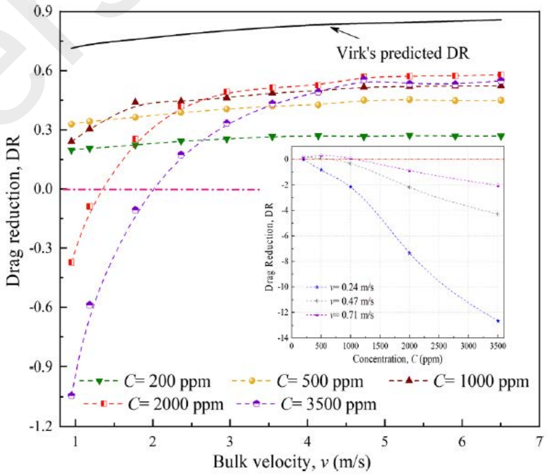

Figure 2.23: DR versus velocity for various XG concentrations in circular tube

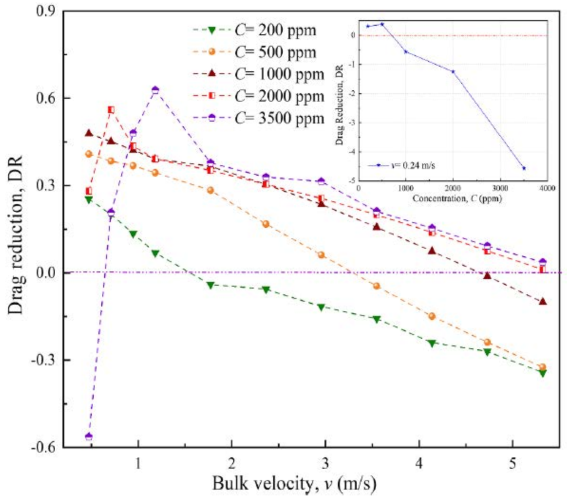

Figure 2.24: DR versus velocity for various XG concentrations in corrugated tube

L. Edomwonyi-Otu et al. (2021) studied xanthan gum (XG) in oil-water mixture flows in circular pips. What they found is in line with the results of other scholars that DR of biopolymers decrease as the percentage of oil present in a mixture increase. They also carried out an experiment to study the drag reduction performance of XG in fresh water. As shown in Figure 2.25 below, DR increases as Re number and concentration increase.

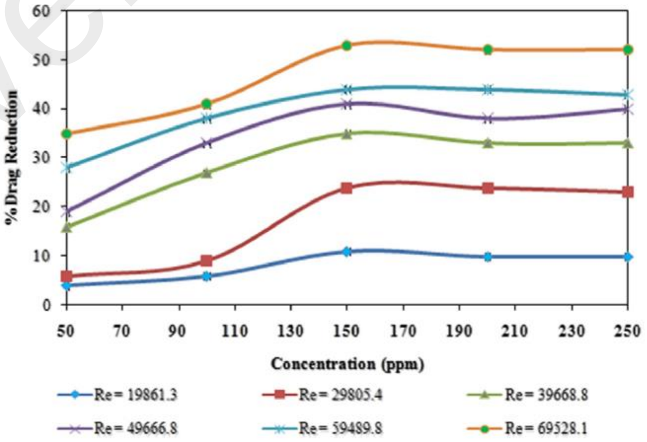

Figure 2.25: DR versus concentration for different Re numbers in 1.2 cm ID pipe

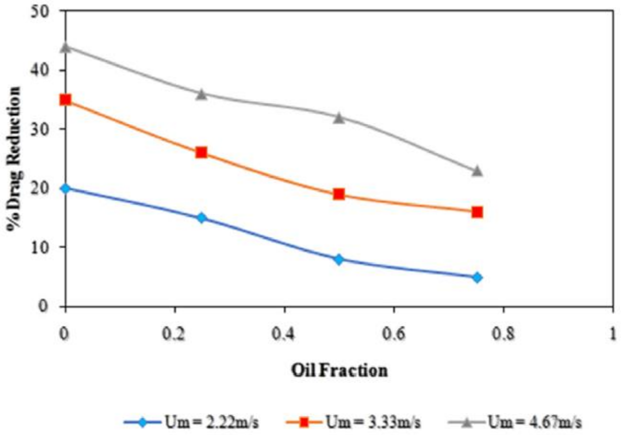

Figure 2.26: DR versus oil ratio for 200 ppm XG at different velocities in 1.2 cm ID pipe

2.5.4 Diutan Gum

dos Santos, Spalenza Caser, Soares, and Siqueira (2020) were the first to study diutan gum's (DG) potential as a flow enhancer in circular piping. They explored several aspects of drag reduction including mechanical degradation, thermal stability, and biodegradation.

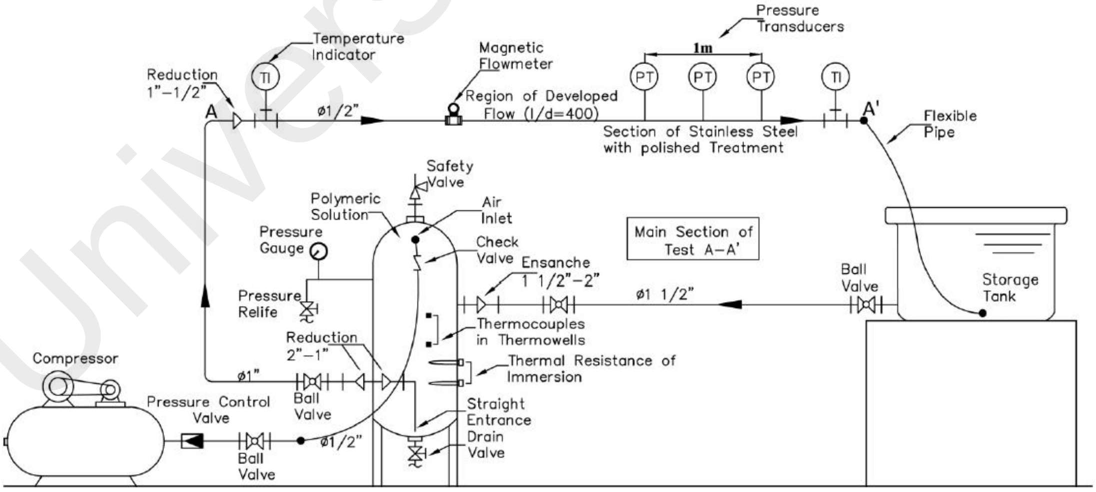

Figure 2.27: Schematic of the test rig used by dos Santos et al. (2020)

To study Mechanical Degradation they carried out tests, using their piping system, for a range of concentrations 25 ppm to 800 ppm. Experiments were carried out at 25°C. DG showed to have high DR of 70% at 800 ppm with strong stability. Because these tests were carried out for just 25 steps, they put DG up for another longer test a Taylor-Couette rotating device at Re of 3560 and using one concentration of 100 ppm. The results were amazing. The test was performed for 72 hours, and the polymer solution did not show any degradation at all.

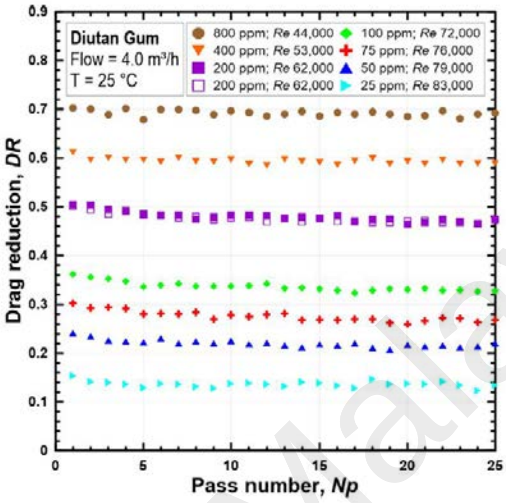

Figure 2.28: Figure 2.29: DR versus number of passes at constant speed for different concentrations

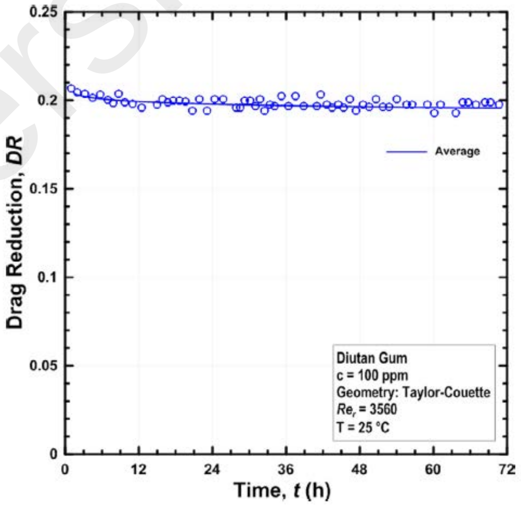

Figure 2.30: DR versus time for DG, 100 ppm

To investigate the thermal stability of DG and XG, dos Santos et al. (2020) made multiple tests with Re 1040 and 100 ppm in their rotating equipment. They cooled the samples from 25 deg C to 5 deg C at 1°C/ min. Then they maintained the temperature at

5 °C for 10 min before reheating back to 25°C. As shown in Figure 2.31 and Figure 2.32, cooling did not have any effect on DR for both biopolymers. In another thermal analysis, they heated the samples at a rate of 1° C /min from 25° C to a maximum temperature of 65° C and in separate tests to 85° C. They maintained the temperature at the maximum temperature for 10 minutes then cooled the samples back to 25° C. DR of XG was significantly decreased while DG was not affected at all.

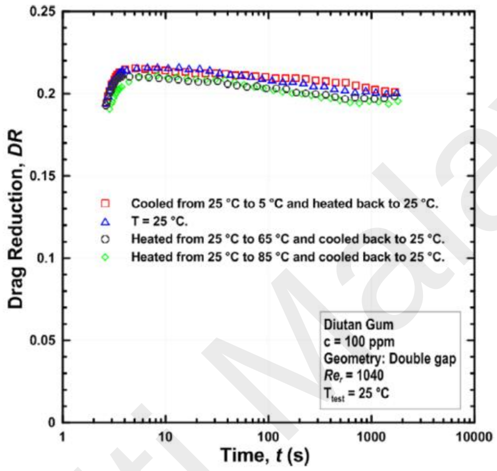

Figure 2.31: DR versus time for DG, 100 ppm, involving heating and cooling cycles

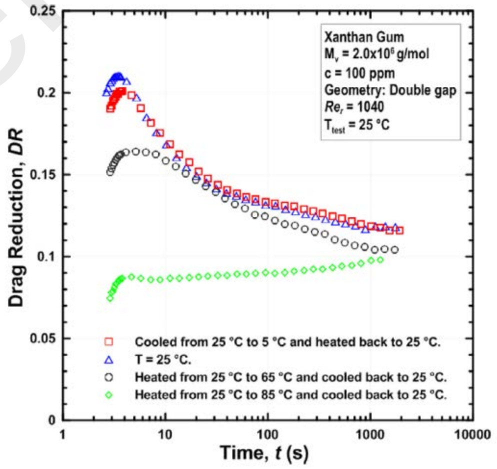

Figure 2.32: DR versus time for xanthan gum, 100 ppm, involving heating and cooling cycles

Finally, they studied biodegradation of DG using 200 ppm samples in the piping system. As shown in Figure 2.33, the DR was about 47% at the end of the first pass. Then they repeated the test on daily basis. After 3 days the DR remained above 40% and after 3 weeks the DR remained positive at about 10%.

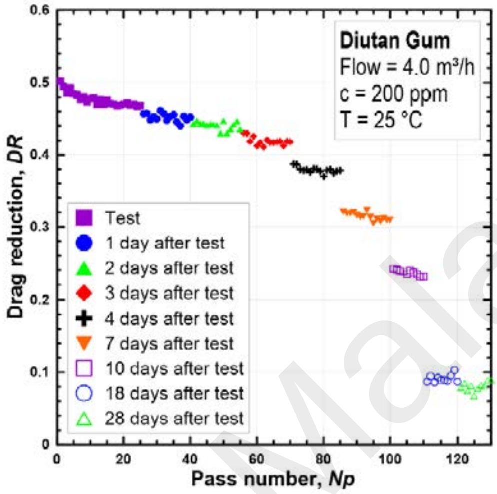

Figure 2.33: DR versus number of passes over 28 days for 200 ppm DG

2.5.5 Carboxymethyl Cellulose

Bin Hasan and Khalid (2017) studied Carboxymethyl cellulose (CMC) ability to reduce drag in a 23.5 mm piping system. They also investigated the drag reduction ability of nanoscale CMC of average size of 43.32 nm to compare it to normal scale CMC. Their experiments used only two flowrates 1 m^3/s and 2m^3/s. As shown in Figure 2.34, for the same flow rate, nano scale DRA offers better drag reduction than normal CMC. For example, DR increased 44% at 1 m^3/s (from 7.258% to 10.484%) and 16% for 2 m^3/s (10.965% to 12.719%).

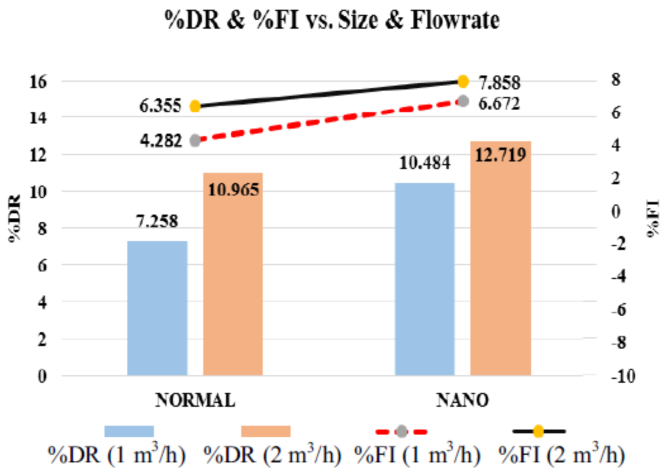

Figure 2.34: Results of Bin Hasan and Khalid (2017) study

2.5.6 Aloe Vera

Bhambri, Narain, and Fleck (2017) tested the drag reduction capability of 600 ppm aloe vera including other DRA using a Taylor-Couette system. They measured DR over a wide range of Re numbers from 40000 to 300000. The best DR they got for aloe vera was about 36% at low Re number but decreased linearly as Re number increased.

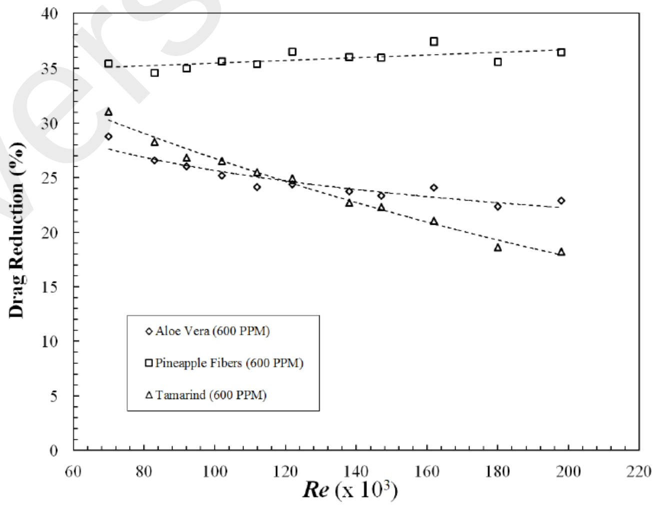

Figure 2.35: DR versus Re number for different polysaccharides

These results partially agree with the works of (Hayder A. Abdul Bari) who tested 100 to 400 ppm aloe vera with a 25.4 mm closed piping system. Hayder A. Abdul Bari (2011) results also show that as Reynold's number increase, DR decrease. But the maximum drag reduction he got is much more that is about 63% at even lower concentration of 400 ppm.

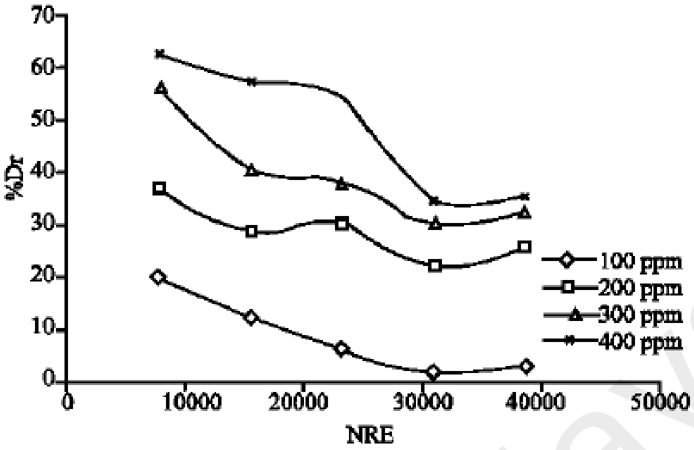

Figure 2.36: %DR versus Re number for different concentrations

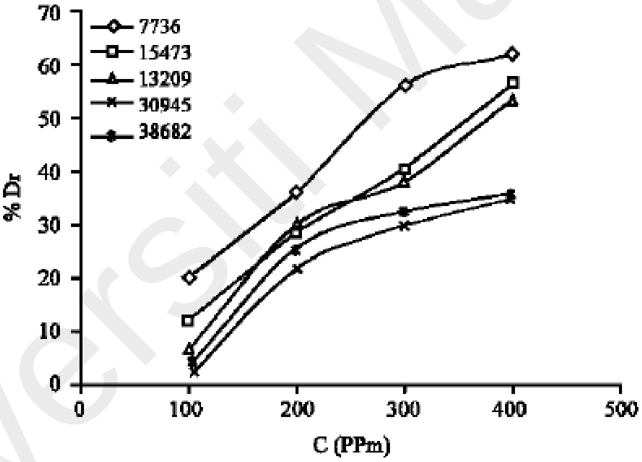

Figure 2.37: %DR versus concentration for different Re numbers

Soares et al. (2019) also studied aloe vera but from a different aspect. Their focus was to investigate the effect of the age of aloe vera leaves on drag reduction.

2.5.7 Biopolymer Blends

Novelli, Ferrari, Vargas, and Loureiro (2019) analyzed drag reduction using binary polymer mixtures. They mixed xanthan gum (XG), polyacrylamide (PAM) and poly(ethyleneoxide) (PEO) with guar gum (GG) to study their effect on drag reduction. They tested different mixture ratios at a range of Re numbers using a rotational rheometer. In the second part of their study, they studied the effect of time on the blends running under fixed Re = 900 for 550 seconds. All solution mixtures prepared of 100 ppm concentration and contained guar gum as one of their constituents. To protect the biopolymers (GG and XG) from biological degradation, the solutions were kept at 6°C. After mixing the mixtures were left for at least 24 hours to hydrate. All experiments were carried out at 20°C.

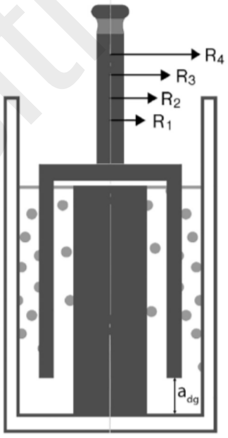

Figure 2.38: Drawing of the Rheometer used by Novelli et al. (2019)

The study concluded that for the GG/XG and GG/polyacrylamide blends, the best drag reduction results achieved by concentrations of 20% GG. However, for GG/poly(ethylene oxide) none of the mixtures performed better than any of the two pure polymers. Novelli et al. (2019) related their results with the molar mass of polymers. They reasoned that blend made up of close molar mass polymers perform best in regard to drag reduction. For example, GG/XG and GG/PAM performed better than GG/PEO.

Table 2.3: Viscosities and average molecular weights of

	GG	XG	PAM	PEO
$[\boldsymbol{\eta}]\ \left({}^{dl}/_{g}\right)$	$\mathbf{13}, 5$	$25, 3$	$5, 71$	$21, 1$
$\overline{M_v}\ (Da)$	$1, 64 \times 10^6$	$1, 96 \times 10^6$	$1, 57 \times 10^6$	$5, 03 \times 10^6$

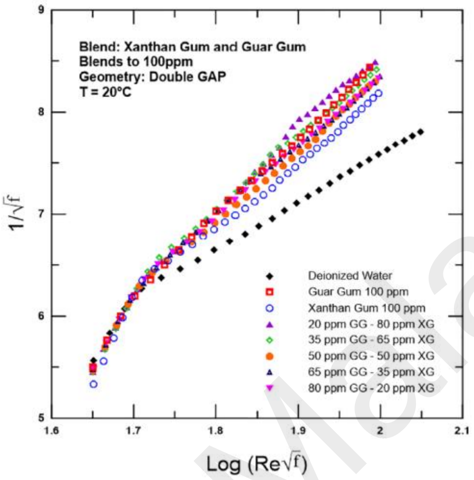

Figure 2.39: Fanning friction factor in Prandtl-Von Karman coordinates for GG and XG mixtures

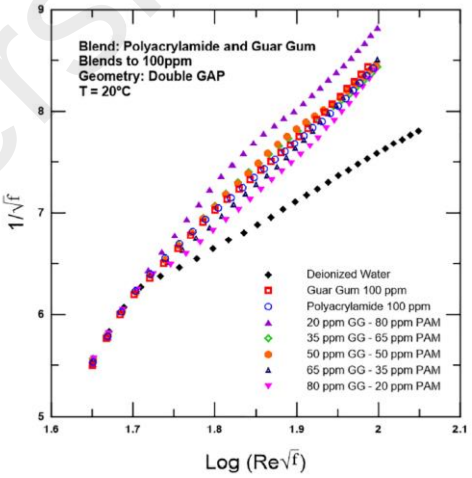

Figure 2.40: Fanning friction factor in Prandtl-Von Karman coordinates for GG and PAM mixtures

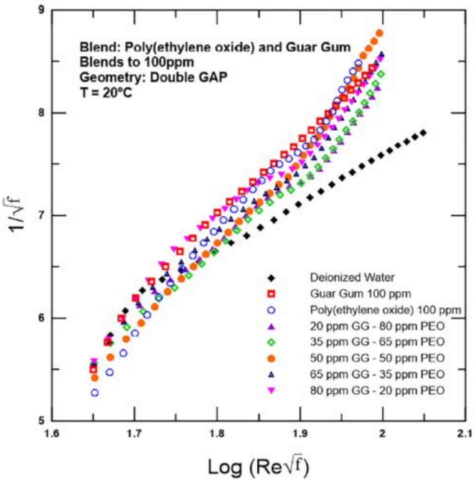

Figure 2.41: Fanning friction factor in Prandtl-Von Karman coordinates for GG and PEO mixtures

Novelli et al. (2019) also concluded that throughout their experiments, the blends resistance to degradation is better than at least one of the two polymers and in the case of GG/polyacrylamide, the blend is better than both polymers when considered alone.

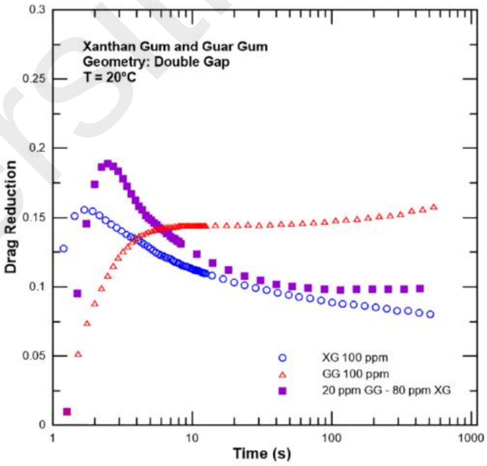

Figure 2.42: DR versus time for XG and GG mixture, 80:20

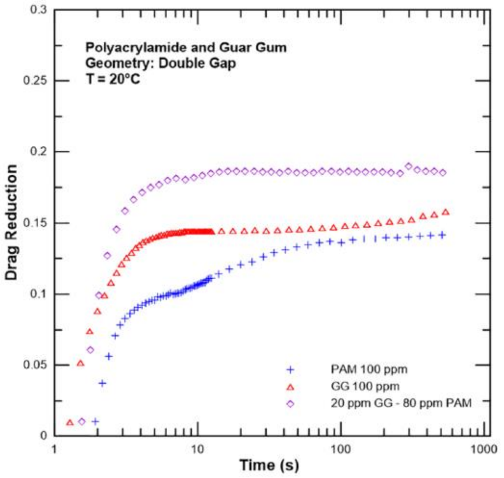

Figure 2.43: DR versus time for PEO and GG mixture, 80:20

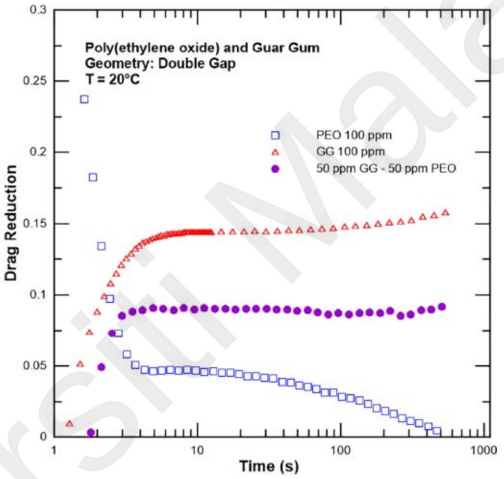

Figure 2.44: DR versus time for PEO and GG mixture, 50:50

Finally, their results agree with the literature in that positive effect is found in all mixture solutions containing at least one rigid polymer, which is in this study the guar gum.

2.6 Summary

This chapter carried about a literature review on drag reduction. It first covered the different theories that exist today on DR, its numerous applications, and various methods. Then it presented an overview of the origins, composition, application, and processing of some of the main biopolymers used today as drag reducing agents. Next it listed the main equations used to analyses to DR and finally it summarized and interpreted some of the recent biopolymers drag reduction studies published by researchers.

CHAPTER 3: METHODOLOGY

3.1 Introduction

This chapter describes in detail the test rig setup, all the tools and equipment utilized in this project and the steps used to carry out the experiments.

3.2 Test Rig and Experimental Setup

The test rig is shown in Figure 3.1. It is made up of twelve main components listed below (See Table 3.1). The fluid gets pumped from the main tank using a centrifugal pump. Then it passes through a magnetic flow meter, a 900 mm heated aluminium test section and finally it returns back to the tank where it gets cooled to the design temperature of 30°C. The inlet and outlet fluid temperatures were obtained using thermocouples (Type K) inserted in the flow. The heated test section in heated by ten 900 W heater coils attached on its outer surface. Downstream the heater coils three grooves were cut along the pipe to house 1.5 mm SS thermowells. These thermowells fixed three Omega type K thermocouples to obtain the wall temperatures at a location 110 mm from the downstream end of the heated section. A differential pressure transmitter is used to record the difference in fluid pressure between two points that are 2440 mm apart and located across the heated section.

1. Stainless Steel Tank

The tank is designed with a hollow wall to function like a heat exchanger. Cold water coming from the cooler circulates within the tank wall to maintain the bulk water temperature of the system to a desired set value. The inner and outer diameters of the tank are 0.5 m and 0.6 m respectively and it can hold about 100 L. It is made of stainless steel and insulated with 3/8" Rubber Foam Thermal Insulation.

Figure 3.1: A photo of the Test Rig

The tank has six pipe connections, two connections connect the tank with the cooler to allow cold water circulation in the hollow wall, while the other four basically connect the tank to the pump supply, main return line, tank circulation return line and finally a drain line.

2. Piping

All the piping of the system is made of stainless steel 304 L expect for the test section that is made of aluminium. The whole piping system is well insulated to minimize heat loss to surroundings.

3. Agitator

The agitator is a mixer whose motor is placed on top of the tank. Its shaft extends into the tank where three rectangular stainless-steel blades 15 cm x 10 cm are attached to it (See Figure 3.2 below). The purpose of the agitator is to properly dilute and mix the master fluid sample (MFS) in the system as well as ensure proper mixing during the experiments. A speed controller can adjust the speed of mixing from a scale of 0 to 93.

Figure 3.2: A photo of the inside of the tank showing the agitator shaft and the SS mixing blades

4. Pump

The pump is of centrifugal type, and it is used to circulate the fluid. Its body and impeller made from stainless steel, and it can deliver a flow of 12 – 48 m³/hr at 50Hz.

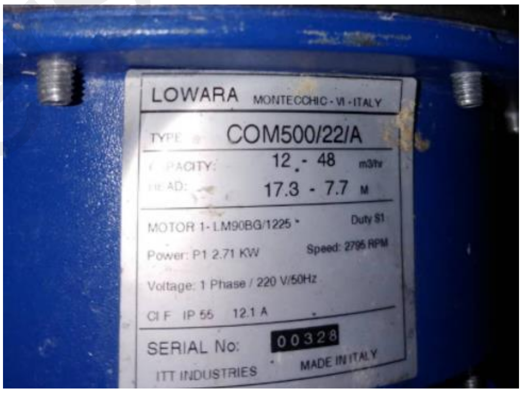

Figure 3.3: Tag Plate of the Pump

5. Variable Frequency Drive

The variable frequency drive (VFD) inverter is used to control the speed of the pump to produce the required different system flowrates as set by the research design. The VFD in located in the main control panel (MCP).

Table 3.1: Specification of the Main Tools and Equipment

S/No.	Equipment Name	Specification
1	Tank	SS, 100 L, Insulation = Insulflex 3/8" Rubber Foam Thermal Insulation
2	Agitator	Tung Lee Electrical, M540-402, 40 W, 90-1400 RPM
3	Agitator Speed Controller	AMS-KB-S, 6-180 W, 220 V, 50/60 Hz
4	Pump	CPM500/22/A (LOWARA), 2.71 KW, 12-48 m^3/hr, 17.3-7.7 m
5	Variable Frequency Drive	Hoffman Muller Inverter, 220 V, 50Hz
6	Flow Meter	Magnetic Type, Foxboro 8000 A Series, Minimum fluid conductivity of 5µs/cm, Flowrate 49 to 946 LPM, –40 to +121°C
7	Flow Transmitter	Magnetic Flow Transmitter, Foxboro IMT25 (DISAI), Accuracy +/- 0.25%, Fluid Velocity Range 0.01 - 10 m/s, -20 to +55 °C, 50/60 Hz
8	Pressure Transmitter	Foxboro IDP10 Electronic Transmitter, Accuracy ±0.05%, Span Limits: 0.5 in H2O and 3000 psid
9	Chiller	JEIO TECH, HX-45H, +3 - 40°C, 4.7 KW Cooling Capacity @20°C/ 2.9 KW @ 5°C, 28 LPM, 50Hz
10	Piping	SS except Test Section Aluminum
11	Thermocouples	Type - K (Omega), 20°C - 150°C
12	Data Logger	MW100 (Yokogawa), PCU-based

6. Magnetic Flow Meter and Transmitter

The inline magnetic flow meter is used to monitor the flowrate of the experiment and it is paired with a flow transmitter with a digital display screen (See Figure 3.4 below).

Figure 3.4: Display Screen of the Flow Transmitter

7. Differential Pressure Transmitter

The differential pressure transmitter (See Figure 3.5 below) is used to record the difference in fluid pressure between two points that are 2440 mm apart.

Figure 3.5: Differential Pressure Transmitter

8. Cooler

The function of the cooler is to control the temperature of the system. It circulates cold water in the tank wall to take away any heat gained by the system e.g., through the pump motor, heating transfer with the ambient atmosphere or through induced heating.

Figure 3.6: Control Panel of the Cooler

9. Data Logger

A PC-based data logger was used to record and display the temperature of five points in the system namely inlet, outlet and three points within the aluminium test section.

Figure 3.7: Data Logger

10. Heaters

Ten heaters each with a capacity of 900 W were attached to the heat transfer test section to supply constant heat flux (See Figure 3.8 below).

Figure 3.8: A photo showing the heaters on the heated test section

11. Main Control Panel

The MCP (See Figure 3.9) houses the VFD as well as the on/off switches of the pump, the heater, and the agitator.

Figure 3.9: A photo of the MCP

Other tools and equipment used in the experiment include:

12. Disintegrator

The pulp disintegrator, which is a quite strong mixer, is used to mix the master fluid samples.

13. Electronic Balance

An electronic balance is used to measure the weight of biopolymers powder.

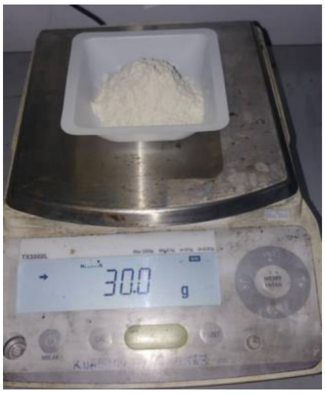

Figure 3.10: Electronic Balance measuring 30 grams of Guar Gum

14. Beakers

Beakers were used to collect distilled water from the temporary tank to prepare the master fluid samples and to fill the main stainless-steel tank as required.

15. Mercury-in-glass thermometer

A thermometer is used to measure the temperature of the fluid during the experiments.

16. Temporary Water Storage Tank

A 200 L temporary tank is used to store distilled water.

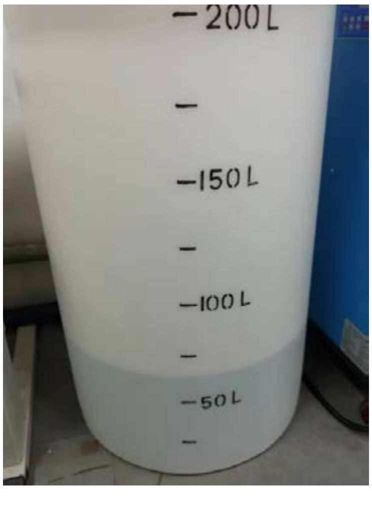

Figure 3.11: Temporary Water Storage Tank

17. Multimeters

Two multimeters were used to measure voltage and current during the experiments to measure the heat flux. Kyoritsu 2017, 600 A/ 600 V Digital Clamp Meter was used to measure the current while the voltage was measured using Agilent U1213A 1000 A/ 1000 V Clamp Meter.

Figure 3.12: Measuring voltage and current using the multimeters

3.3 Experimental Procedure

This section describes in detail the step-by-step procedure carried out for all the experiments of this research.

3.3.1 Material

The Guar Gum used in this project is sourced from Sigma-Aldrich, USA, while the Gum Arabic is sourced from Merk - Germany.

3.3.2 Distilled Water Production

To remove any potential interference from tap water that would cause fluctuations in results, distilled water was used in all experiment of the project. A water distiller (See Figure 3.13) was used to produce distilled water at a rate between 0.9 L/ hr and 4.8 L/hr. The tap water supply valve was carefully adjusted to achieve a good production rate greater than 4 L/hr. The produced water is delivered into a temporary container then manually transferred to a 200 L temporary plastic water storage tank. Each concentration required 100 L of distilled water. Also, 100 L of water was used to flush the system before starting the experiments and about 50 L were used to flush the system in between different experiments of different concentrations. In total, considering also few tests runs that were carried out before starting the main experiments, about 1000 L of distilled water was used to complete this research and it took about 250 hours to produce.

Figure 3.13: Water Distiller

3.3.3 System Flushing

Before stating experimental runs, the piping was flushed with 100 L of tap water for 15 minutes at full pump speed. Then, water was drained, and the stainless-steel tank is refilled with 100 L of distilled water for another flush. Subsequently, between experimental runs the system got a 15-minute flush with 100 L tap water then 50 L distilled water to ensure that traces from one experiment would not affect the results of another experiment.

Figure 3.14: Filling the main tank with distilled water

3.3.4 Distilled Water Run, Part 1, Without Heating

The first experiment was carried out with distilled water (without any additives). This served as a baseline for other experiments that included DRA's. Initially the main tank was filled with 100 L of distilled water and then the pump started and adjusted to full speed. When the temperature of the water in the stainless-steel tank reached ±0.5°C from the design temperature 30°C, the cooler was started to maintain the temperature. The pump speed was reduced by reducing the frequency of the VFD from the control panel until the flow transmitter displayed an average flowrate within ±2% of the first point which is 292.17 LPM (equivalent to flow speed of 3.6 m/s). At that point the system was left for at least 3 minutes to stabilize. Then five readings were logged into a spreadsheet:

- Tank water temperature, manually measured using a mercury thermometer
- Inlet Temperature, recorded from the data logger display screen
- Frequency of the inverter
- Average flowrate
- Average differential pressure

Figure 3.15: Adjusting the frequency of the VFD

Next the flow speed was decreased until the flowrate of the next point was reached (±2%). Again, the system was left for a minimum of 3 minutes to get to steady state and then the five readings were recorded accordingly. The process was repeated for thirteen different flow speeds from 0.4 m/s to 3.6 m/s as per the research design. At low fluid velocities, less heat was transferred from the pump motor into the fluid therefore the cooler was turned off to maintain the inlet temperature at 30°C.

3.3.5 Distilled Water Run, Part 2, With Heating

In the second part of the experiment, the heater is turned on and set to 35% of its maximum power, using a controller, to provide a constant power flux of 3400 W while the pump was set to operate at full speed. The cooler was turn back on and initially set to 18°C. The system was left in this condition for at least 90 minutes until steady state conditions were achieved. The pump speed was reduced by adjusting the frequency of the inverter until the flow transmitter displayed an average flowrate within ±2% of the first point which is 227.25 LPM (equivalent to flow speed of 2.8 m/s). At that point the system was left for at least 3 minutes to stabilize. Then eleven readings were logged into a spreadsheet as follows:

- Tank water temperature, manually measured using a mercury thermometer
- From the data logger display screen: Inlet temperature, outlet temperature and three temperature points located within the test section and just downstream the heater rods.
- Frequency of the inverter
- Average flowrate
- Average differential pressure
- Current and Voltage

Figure 3.16: Controller of Heaters set to 35%

Then the flow speed was decreased and similarly, the process was repeated for the remaining six flow speeds from 0.4 m/s to 2.8 m/s as per the research design. Throughout all experiments, the agitator mixer was switched on and its speed controller was set to 75 to ensure adequate mixing of the fluids and to provide better heat transfer within the tank.

3.3.6 Mixture 1: 300 ppm Mixture, 12.5% GG + 87.5% GA

Throughout all the experiments of this project 300-ppm concentrations were used. To create a 300-ppm mixture, we would need 300 g per 1 m^3 volume. So, for 100 L, the total weight of DRA mixture to be used is 30 g. Fluid 1 includes 12.5% GG and 87.5% GA so to prepare a 300-ppm concentration, 3.75 g and 26.25 g were needed from GG and GA respectively.

Figure 3.17: Measuring GG to prepare an MFS

First, 2000 ml of distilled water at ambient temperature were measured by a beaker and poured into the pulp disintegrator container. Next the required amount of GG was measured using an electronic balance and then added to the water. The sample is then mixed in the disintegrator for 3 full cycles of 5000 revolutions until the mixture became totally homogenous. Similarly, the required amount of GA was obtained and then added into the container of the disintegrator. The mixture was mixed for another 3 full cycles of 5000 revolutions to obtain a 15000-ppm master fluid sample.

Figure 3.18: Pouring distilled water in the disintegrator to prepare an MFS

The MFS is then added to 98 L of distilled water (to form the required 100 L) in the main SS tank. Next the agitator mixed the blend for about 30 minutes until it became homogenous, and the fluid is left in the tank for at least 12 hours for proper hydration.

The next day, the pump started and adjusted to full speed. When the temperature of the water in the main tank reached ±0.5°C from the design temperature, the cooler was started to maintain the temperature. The pump speed was reduced by reducing the frequency of the VFD from the control panel until the flow transmitter displayed an average flowrate within ±2% of the first point which is 292.17 LPM (equivalent to flow speed of 3.6 m/s). From there the same procedure used for the Distilled Water Runs parts 1 and 2 (With and without heating) was followed until all the required data was collected.

3.3.7 Other Concentrations

The same process is repeated for four more MFS's as per Table 3.2 below.

Table 3.2: Ratio and Weight of Polymers per each Master Fluid Sample

Fluid	Water Volume (L)	Concentration (ppm)	%GG	%GA	GG Weight (g)	GA Weight (g)
1	100	300	12.5	87.5	3.75	26.25
2	100	300	25	75	7.50	22.50
3	100	300	50	50	15.00	15.00
4	100	300	100	0	30.00	0.00
5	100	300	0	100	0.00	30.00

3.4 Summary

This chapter presented an overview over the test rig, tools, equipment and material used in this study and discussed in detail the experimental procedures used. The velocity range in part 1 of the experiments was from 0.4 m/s – 3.6 m/s while in the heating part velocities considered from 0.4 m/s – 2.8m/s. In all runs (with or without heating), the temperature of fluid in the tank was maintained at 30°C ±0.5°C.

CHAPTER 4: RESULTS AND DISCUSSION

4.1 Introduction

This chapter presents and analyses the results of all experiments of this study. All runs were carried out using 300 ppm concentrations.

4.2 Water Run Results

The friction factor of the experimental results of distilled water as well as several empirical equations are plotted in Figure 4.1. The experimental data, calculated using Darcy friction factor equation (Eq 2.5), is compared to the empirical equations of Colebrook, Haaland, Petukhov and Balsius (See Equations 2.6 to 2.9 respectively). At low velocities, the experimental results are in big deviation with the standard equations. For example, there is a difference of 97.16% at 0.4 m/s and 45.59% at 0.6 m/s when comparing the experimental data to the results of Colebrook. The gap quickly reduces to 20.49% at 1 m/s and the results become pretty matching with Colebrook and Haaland with less than 3% difference for velocities greater than or equal to 2.8 m/s.

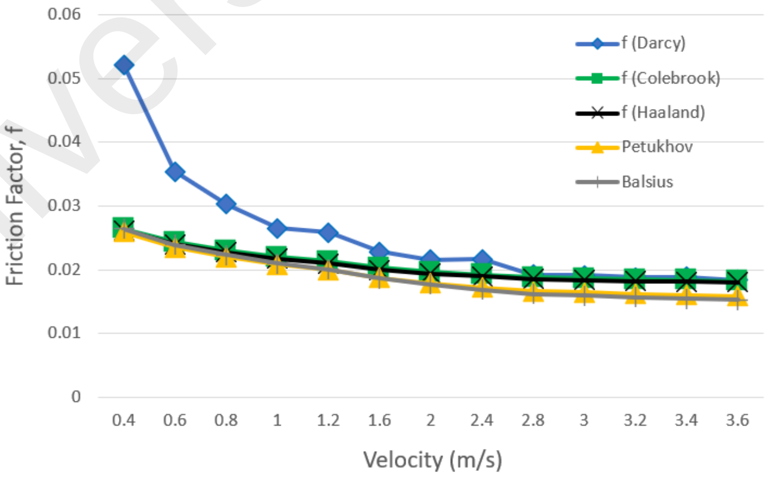

Figure 4.1: Comparing Friction Factor Results of Distilled Water with Standard Empirical Correlations

Friction factor (f) and pressure drop results as a function of velocity are plotted in Figure 4.2 and Figure 4.3 respectively. The results of the "before heating" and "after heating" runs are almost identical. In other words, for distilled water, heating has no effect on friction factor or pressure drop. However, friction factor decreases as velocity increases until it almost stabilizes at high speeds while pressure drop increase with increasing water velocity.

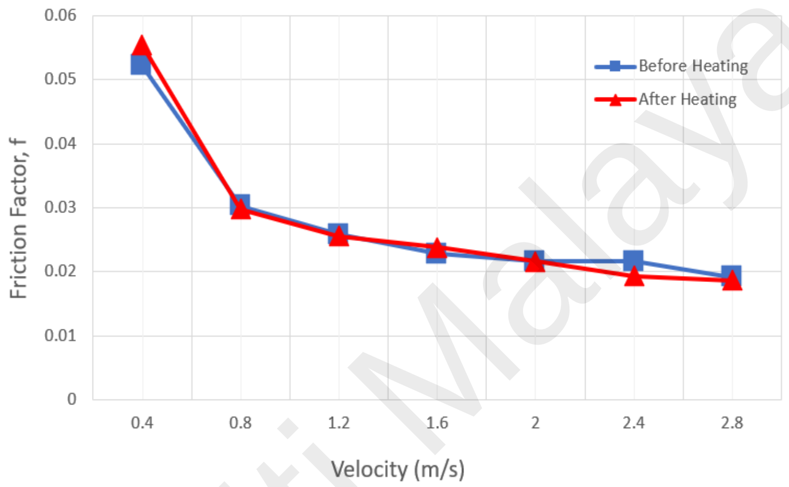

Figure 4.2: Distilled Water Friction Factor Results plotted as a function of Velocity "Before Heating" and "After Heating"

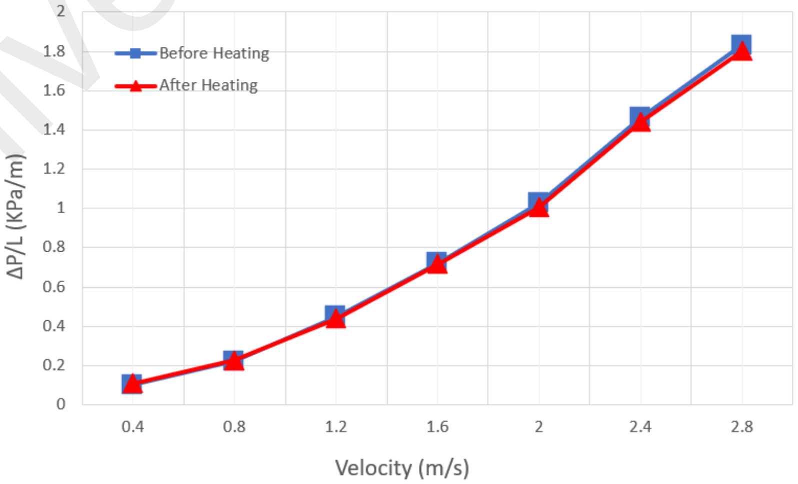

Figure 4.3: Distilled Water Pressure Drop Results plotted as a function of Velocity "Before Heating" and "After Heating"

4.3 Effect of Biopolymers Mixing Ratio

In order to study the effect of mixing ratio of GG and GA on drag reduction, several experiments were conducted using the same overall concentration of 300 ppm. Total five fluids were studied. Two composed of only one DRA, GG, and GA, while the other three were mixtures of these two polymers. The composition ratio of the mixtures is as per Table 3.2. For each fluid, two experiments done. One without heating while the other experiment was carried out after the fluid was heated for about 90 min and then the data were collected during heating.

4.3.1 Friction Factor

Figure 4.4 and Figure 4.5 display the friction factors results of all the experiments of this study. The results show a similar trend for both “before heating” and “after heating” experiments. Friction factor decreases as velocity increase. Also, the data is pretty similar for all fluids at low speeds, but for velocities greater than 1 m/s it become distinct. For example, for the “before heating” case at 3.6 m/s, GG 100% got the lowest f of 0.0127, followed by GG 50% at 0.0142, GG 25% at 0.0149, GG 12.5% at 0.0165 and distilled water at 0.0184. The friction factor of GA 100% was the highest at 0.0190. Therefore, we can say that as the ratio of GG in the fluid increase, the fiction factor decreases.

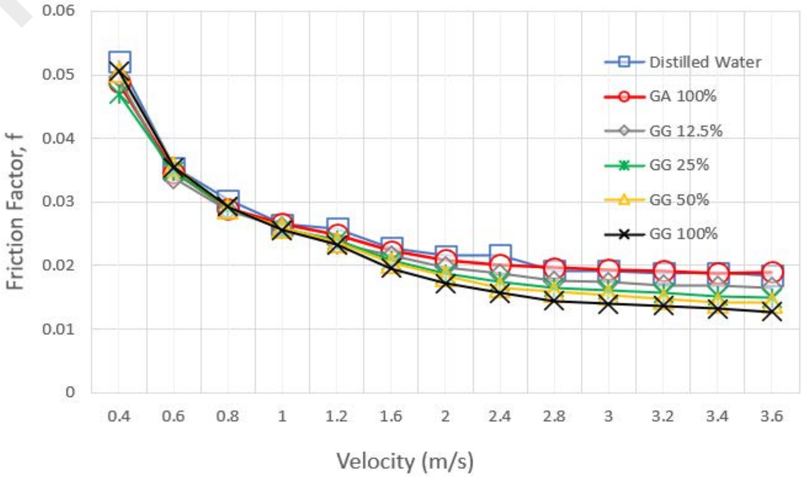

Figure 4.4: Friction Factor Results of all Fluids at different Velocities “Before Heating”

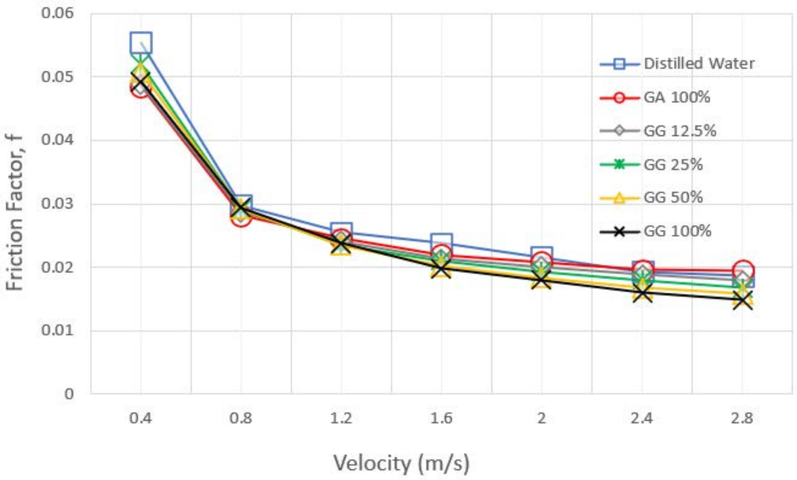

Figure 4.5: Friction Factor Results of all Fluids at different Velocities "After Heating"

4.3.2 Pressure Drop

Figure 4.6 and Figure 4.7 compile the pressure drop results of all the experiments of this research. For all fluids and over the whole range of velocities, pressure drop increase as velocity increase. For the experiments made "before heating", all fluids show a slight increase in pressure drop at low speeds (≤ 1.2 m/s). Then for fluid velocities between 1.2 m/s and 2.8 m/s, the data become distinct and display a rapid increase. And finally at higher velocities the pressure drop continues to increase but at slower rate. For the "before heating" runs at 3.6 m/s, GG 100% got the lowest pressure drop of 1.997 Kpa/m, followed by GG 50% at 2.207 Kpa/m, GG 25% at 2.323 Kpa/m, GG 12.5% at 2.525 Kpa/m and distilled water at 2.853 Kpa/m. The pressure drop of GA 100% was the highest at 2.898 Kpa/m. For the experiments made during heating, the results show a very similar trend. Therefore, for both "heating" and "not heating" experiments and for velocities greater than 1.2 m/s, we can say that as the ratio of GG in the fluid increase, the pressure drop decrease.

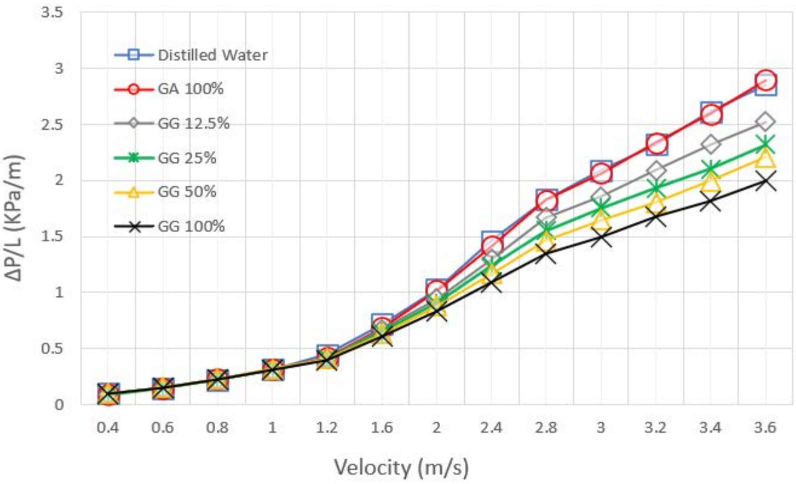

Figure 4.6: Pressure Drop Results of all Fluids at different Velocities "Before Heating"

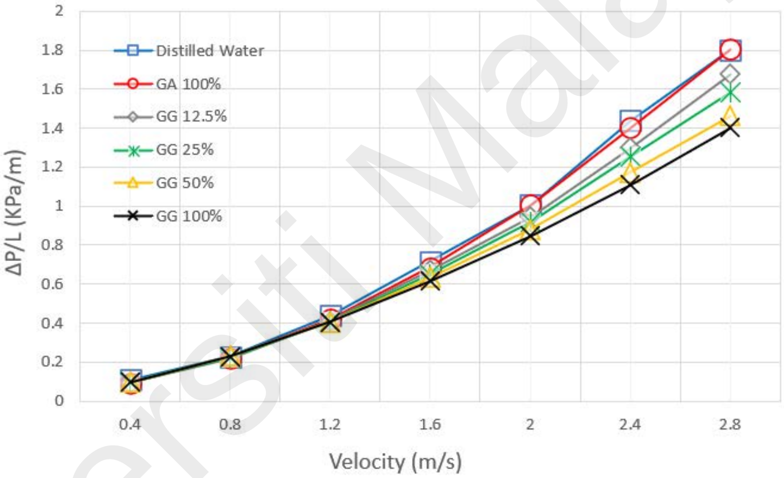

Figure 4.7: Pressure Drop Results of all Fluids at different Velocities "After Heating"

4.3.3 Drag Reduction

Figure 4.8 and Figure 4.9 present the drag reduction results of all the experiments of this study. For velocities less than or equal to 0.8 m/s, DR decreases as velocity increase. While for velocities greater than or equal to 1 m/s, it is evident that the more GG present in the fluid the better the drag reduction. Adding as little as 12.5% concentration ratio of GG to GA significantly improves its DR performance. The maximum drag reduction is offered by GG 100% solution at 3.6 m/s at 30.03%. While, at the same velocity, GG 50%

achieved 22.65% followed by GG 25% at 18.58%, GG 12.5% at 11.50% and finally GA 100% got a negative value of -1.57% DR.

Figure 4.8: Drag Reduction Results of all Fluids at different Velocities "Before Heating"

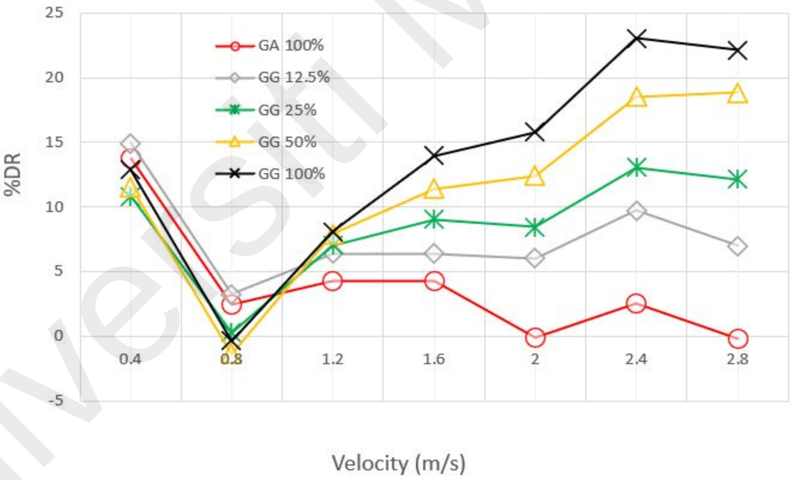

Figure 4.9: Drag Reduction Results of all Fluids at different Velocities "After Heating"

4.4 Effect of Heating

This section presents the experimental results of each fluid separately to study the effect of heating on friction factor, pressure drop and drag reduction. As per Figures 4.10 to 4.19, heating does not seem to have any effect on friction factor or on pressure drop for all fluids. The data collected before heating and after heating are almost identical.

Pressure drops increase with velocity while friction factor decreases quickly between 0.4 m/s to 0.8 m/s then it continues to decrease but at a much lower rate.

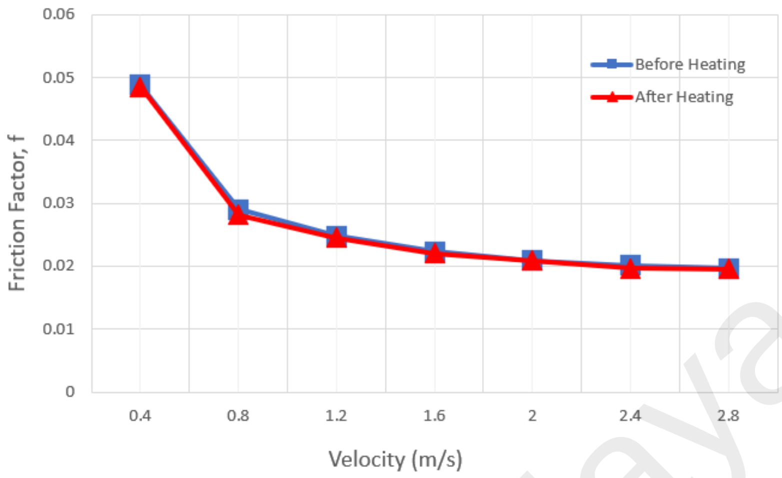

Figure 4.10: GA 100% Friction Factor Results plotted as a function of Velocity "Before Heating" and "After Heating"

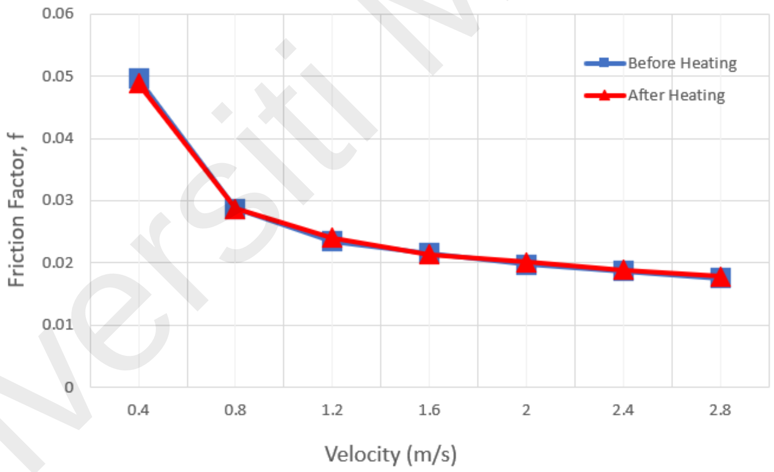

Figure 4.11: GA 87.5% + GG 12.5% Friction Factor Results plotted as a function of Velocity "Before Heating" and "After Heating"

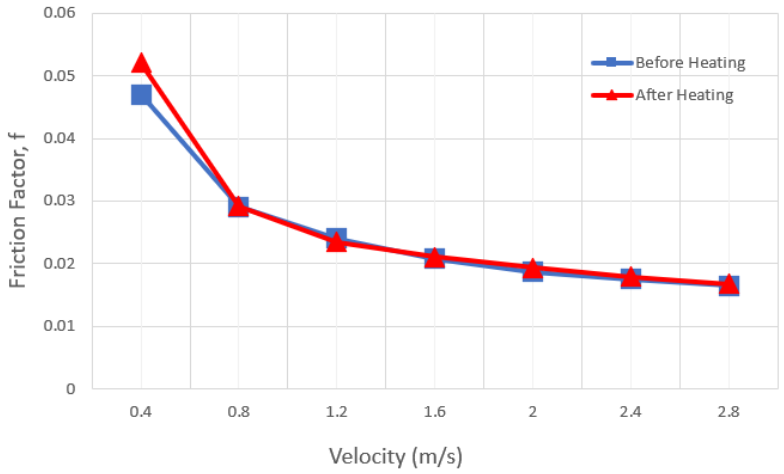

Figure 4.12: GA 75% + GG 25% Friction Factor Results plotted as a function of Velocity “Before Heating” and “After Heating”

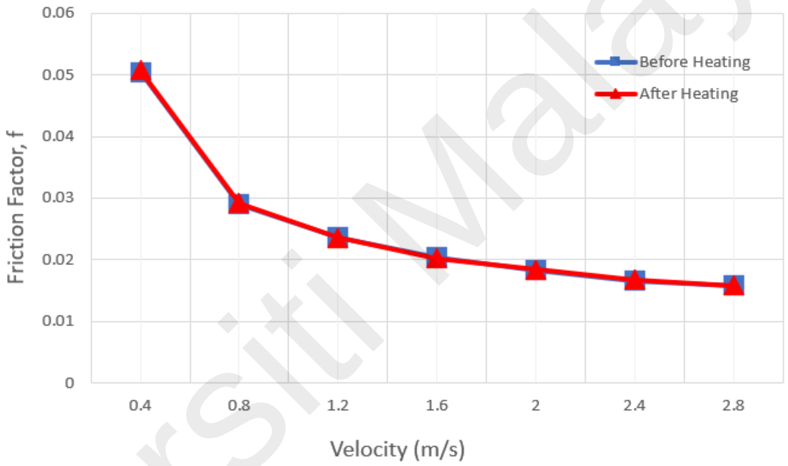

Figure 4.13: GA 50% + GG 50% Friction Factor Results plotted as a function of Velocity “Before Heating” and “After Heating”

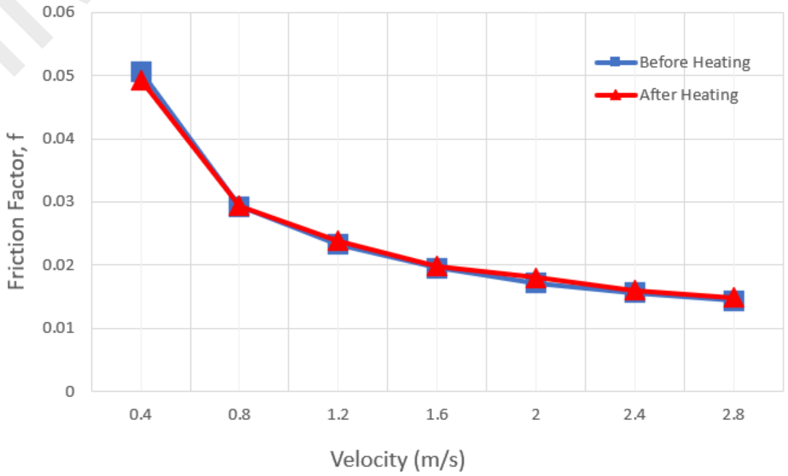

Figure 4.14: GG 100% Friction Factor Results plotted as a function of Velocity “Before Heating” and “After Heating”

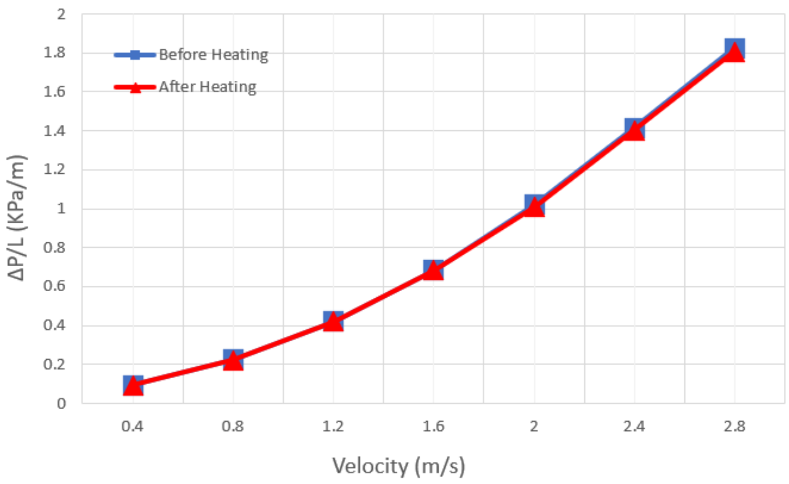

Figure 4.15: GA 100% Pressure Drop Results plotted as a function of Velocity “Before Heating” and “After Heating”

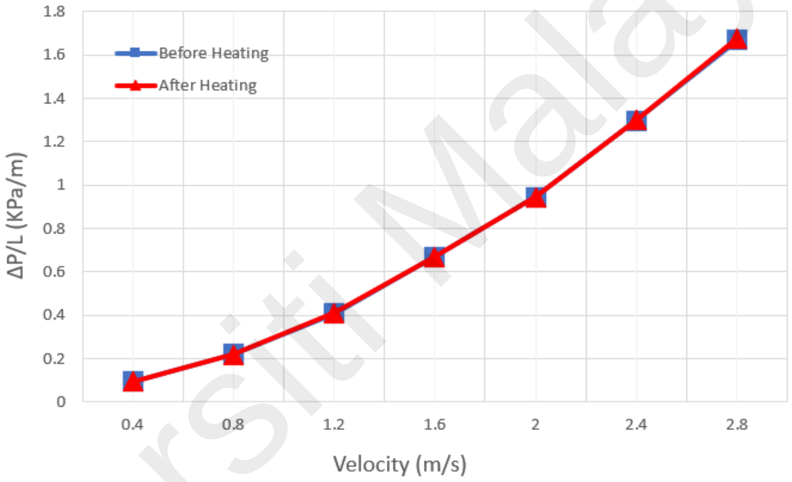

Figure 4.16: GA 87.5% + GG 12.5% Pressure Drop Results plotted as a function of Velocity “Before Heating” and “After Heating”

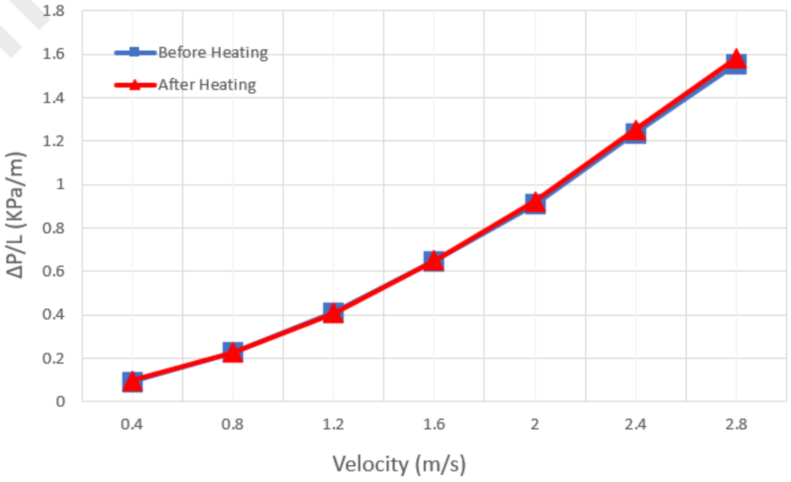

Figure 4.17: GA 75% + GG 25% Pressure Drop Results plotted as a function of Velocity “Before Heating” and “After Heating”

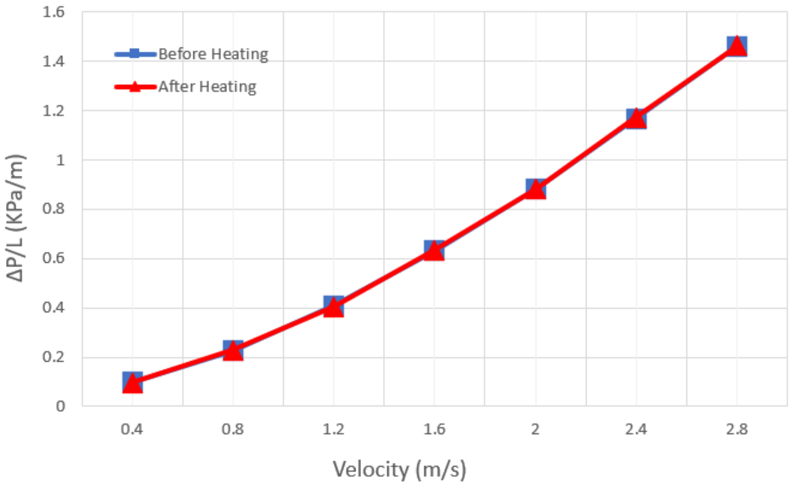

Figure 4.18: GA 50% + GG 50% Pressure Drop Results plotted as a function of Velocity "Before Heating" and "After Heating"

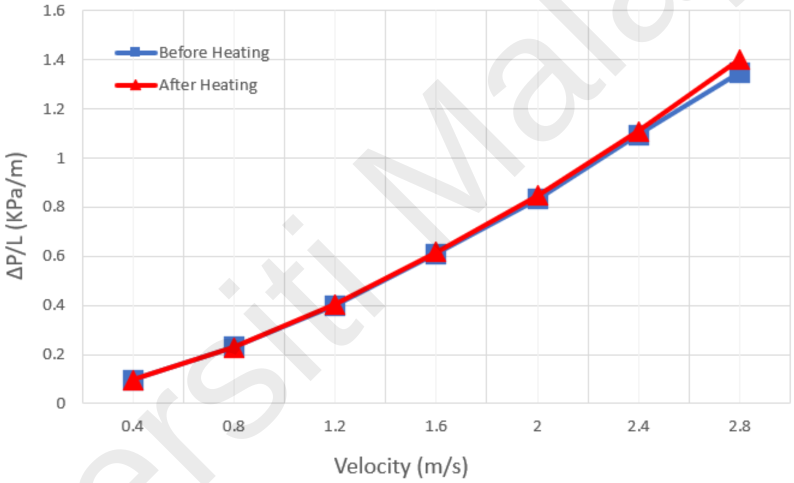

Figure 4.19: GG 100% Pressure Drop Results plotted as a function of Velocity "Before Heating" and "After Heating"

While on the other hand, heating has an obvious impact on drag reduction. Considering Figures 4.20 to 4.24 below, velocity 1 m/s seems to separate all the plots for all fluids into two parts. In first part which is for low velocities, heating improves DR. For example, for GG 50% fluid at 0.4 m/s, the DR was 2.05% without heating and it jumped to 11.55% with heating. That's more than 500% improvement. While for higher velocities in the second part, heating actually reduces DR. On average, heating reduced DR for GA 100% solution by 70.10%, for GG 12.5% solution by 19.57%, for GG 25% solution by 17.10%, for GG 50% solution by 9.35%, and finally for GG 100% solution by 15.73%.

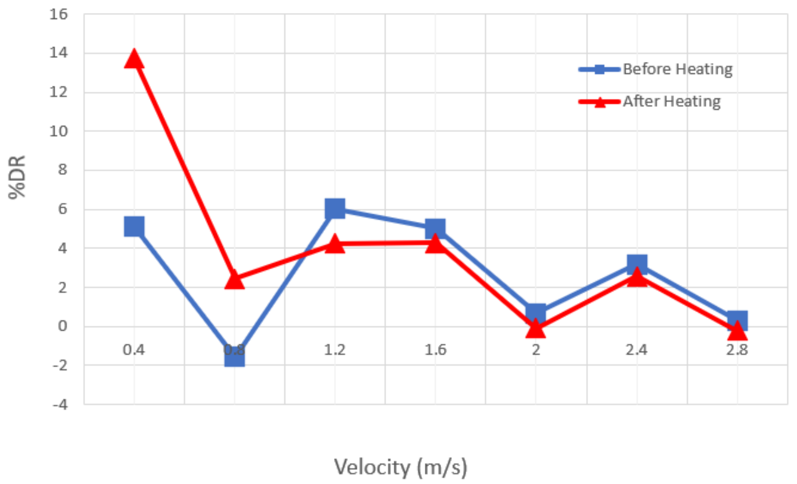

Figure 4.20: GA 100% Drag Reduction Results plotted as a function of Velocity “Before Heating” and “After Heating”

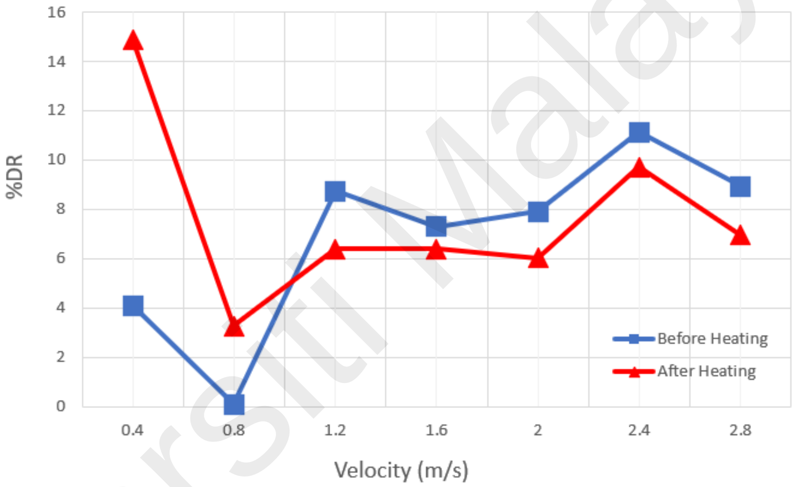

Figure 4.21: GA 87.5% + GG 12.5% Drag Reduction Results plotted as a function of Velocity “Before Heating” and “After Heating”

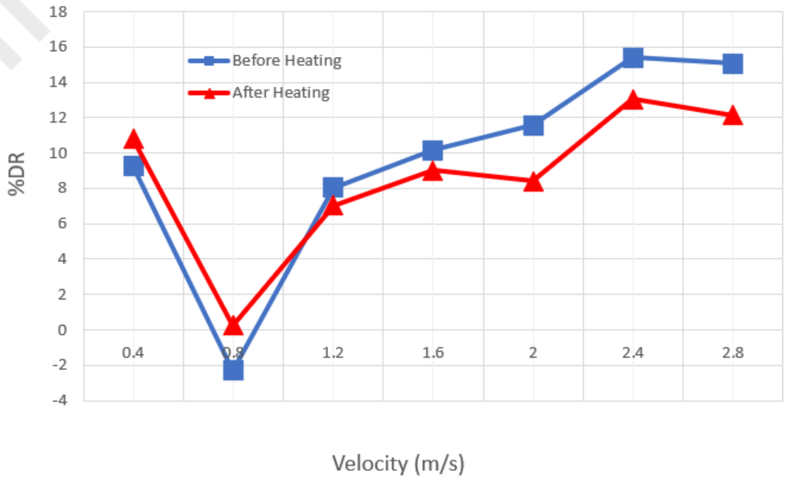

Figure 4.22: GA 75% + GG 25% Drag Reduction Results plotted as a function of Velocity “Before Heating” and “After Heating”

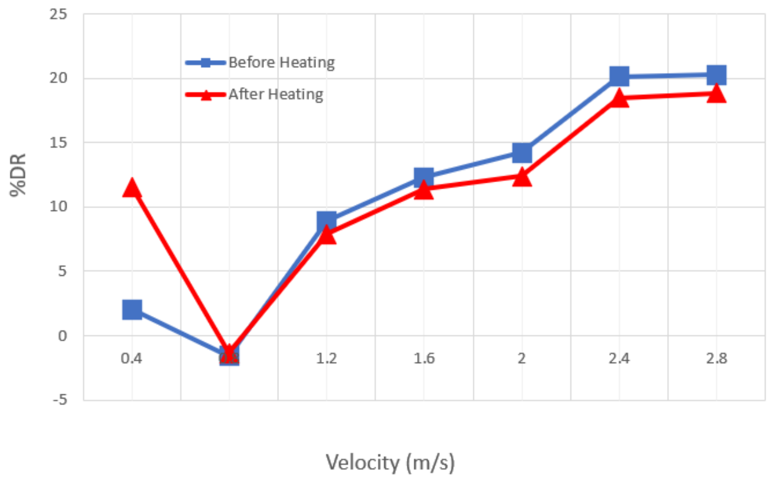

Figure 4.23: GA 50% + GG 50% Drag Reduction Results plotted as a function of Velocity "Before Heating" and "After Heating"

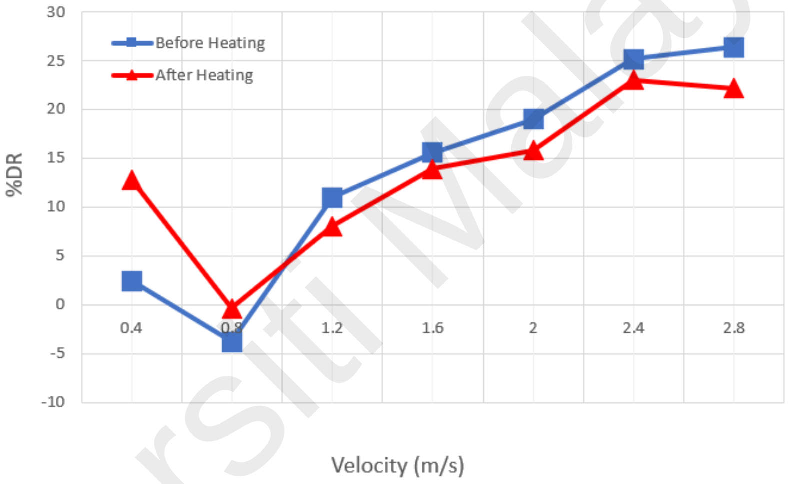

Figure 4.24: GG 100% Drag Reduction Results plotted as a function of Velocity "Before Heating" and "After Heating"

4.5 Challenges associated with the experiments

4.5.1 Fluctuations of Readings

The main concern associated with this study was the fluctuation of readings. It is still clear what is the cause of these fluctuations, however, it is evident that the presence of air bubbles in the system has a direct impact on the stability of readings. First, the experimental works were started using 80 L. This volume of water in the system meant that during the runs, the return line in the tank was not submerged in water and this allowed more air bubbles to be sucked by the pump and cause too much fluctuation in the flow rate and hence the pressure readings. To go around this, we decided to run the experiments on 100 L to ensure that the return line is submerged in water. As a result, fluctuations were reduced but the stability problem was still there. To ensure that the readings collected accurately reflect the average, all readings from all instruments were video recorded using a handphone camera. Then the videos were reviewed to identify the minimum and maximum results and the average is calculated accordingly. The display screen of the flow transmitter and pressure transducer were video recorded for at least 10 sec for each flow and pressure reading respectively. While the data logger display was recorded for at least 15 sec.

4.5.2 Duration of Experiments

Another concern related to the experiments of this study is the fact that the runs are time consuming. First, to produce the required 100 L distilled water it took about 4 days. This led to some idle days awaiting the availability of distilled water. The issue was bypassed later by sourcing water from other labs. Then, once the MFS is prepared and mixed for 30 minutes in the main SS tank, it was left for at least 12 hours for hydration. And finally, each experiment, including parts one and two, took on average 10 hours of focused activity per each fluid.

4.6 Summary

This chapter started by validating the experimental results of the test rig. Distilled water results were compared with the existing standard correlations. Then the test results of different biopolymer samples were presented and discussed in detail. The best drag reduction of 30.03% is achieved by GG 100% fluid at the highest velocity of 3.6 m/s. Also, for velocities greater than 1 m/s, heating was found to reduces drag reduction by 9.35% - 70.1% while it has negligible impact over friction factor and pressure drop.

Another important conclusion is that the higher the ratio of GG in a fluid the better the drag reduction. Finally, some concerns with the experimental works were discussed.

CHAPTER 5: CONCLUSION

5.1 Conclusion

This study presented an overview of some of the recent studies on biopolymers and their effectiveness with respect to drag reduction. Then, mixtures made up of guar gum and gum Arabic were explored using a close conduit system to test their ability to reduce drag. We concluded that for GG/ GA mixtures, the higher the ratio of GG in a fluid the better the drag reduction. The DR performance of GA can be considerably improved by adding slight concentration of 12.5% of GG. The best drag reduction of 30.03% is achieved by GG 100% fluid followed by GG 50% fluid at 22.65%. Both of these results were achieved at 3.6 m/s fluid velocity. Another important conclusion was that heating reduces drag reduction for velocities greater than 1 m/s but it has no effect on friction factor and pressure drop.

5.2 Recommendations for Future Works

Based on the literature review and on the findings of this study, the following is recommended for future research:

- Investigating the biodegradation of GG and GA
- Investigating the mechanical degradation of the biopolymers
- Exploring different biopolymer mixtures
- Studying the effect of salt on the mixtures ability to reduce drag
- Studying the behavior of the GG/ GA mixture on oil/ water flow
- Studying the effect of low temperature on DR performance of polymer mixtures
- Conducting economic analysis of using different biopolymers for different applications
- Adding an air separator in the test rig
- Taking out the elbows from the pump suction line

REFERENCES

Abdulbari, H. A., Yunus, R. M., Abdurahman, N. H., & Charles, A. (2013). Going against the flow—A review of non-additive means of drag reduction. *Journal of Industrial and Engineering Chemistry, 19*(1), 27-36. doi:https://doi.org/10.1016/j.jiec.2012.07.023

Abu Elella, M. H., Goda, E. S., Gab-Allah, M. A., Hong, S. E., Pandit, B., Lee, S., . . . Yoon, K. R. (2021). Xanthan gum-derived materials for applications in environment and eco-friendly materials: A review. *Journal of Environmental Chemical Engineering, 9*(1), 104702. doi:https://doi.org/10.1016/j.jece.2020.104702

Al-Sarkhi, A. (2010). Drag reduction with polymers in gas-liquid/liquid-liquid flows in pipes: A literature review. *Journal of Natural Gas Science and Engineering, 2*(1), 41-48. doi:https://doi.org/10.1016/j.jngse.2010.01.001

Asidin, M. A., Suali, E., Jusnukin, T., & Lahin, F. A. (2019). Review on the applications and developments of drag reducing polymer in turbulent pipe flow. *Chinese Journal of Chemical Engineering, 27*(8), 1921-1932. doi:https://doi.org/10.1016/j.cjche.2019.03.003

Bhambri, P., Narain, R., & Fleck, B. (2017). Drag Reduction Using Polysaccharides in a Taylor-Couette Flow. *Polymers, 9*(12), 11. doi:10.3390/polym9120683

Bin Hasan, M. L., & Khalid, M. N. B. (2017). Preparation of Nano-Scale Biopolymer Extracted from Coconut Residue and Its Performance as Drag Reducing Agent (DRA). In A. Hasan, A. A. Khan, M. A. Mannan, C. N. Hipolito, N. M. Sutan, A. K. H. Othman, M. R. Kabit, & N. A. Wahab (Eds.), *9th International Unimas Stem Engineering Conference* (Vol. 87). Cedex A: E D P Sciences.

Brostow, W. (2008). Drag reduction in flow: Review of applications, mechanism and prediction. *Journal of Industrial and Engineering Chemistry, 14*(4), 409-416. doi:https://doi.org/10.1016/j.jiec.2008.07.001

Çengel, A. J. G. Y. A. (2015). *Heat and Mass Transfer - Fundamentals & Applicaitons* (Fifth ed.): McGrawHill Education.

dos Santos, W. R., Spalenza Caser, E., Soares, E. J., & Siqueira, R. N. (2020). Drag reduction in turbulent flows by diutan gum: A very stable natural drag reducer. *Journal of Non-Newtonian Fluid Mechanics, 276*, 104223. doi:https://doi.org/10.1016/j.jnnfm.2019.104223

Dosumu, A. I., Edomwonyi-Otu, L. C., Yusuf, N., & Abubakar, A. (2020). Guar Gum as Flow Improver in Single-Phase Water and Liquid–Liquid Flows. *Arabian Journal for Science and Engineering, 45*(9), 7267-7273. doi:10.1007/s13369-020-04429-2

Edomwonyi-Otu, L., Dosumu, A., & Yusuf, N. (2021). Effect of oil on the performance of biopolymers as drag reducers in fresh water flow. *Heliyon, 7*, e06535. doi:10.1016/j.heliyon.2021.e06535

Edomwonyi-Otu, L. C., Dosumu, A. I., & Yusuf, N. (2021). Effect of oil on the performance of biopolymers as drag reducers in fresh water flow. *Heliyon, 7*(3), e06535. doi:https://doi.org/10.1016/j.heliyon.2021.e06535

George, A., Shah, P. A., & Shrivastav, P. S. (2019). Guar gum: Versatile natural polymer for drug delivery applications. *European Polymer Journal, 112*, 722-735. doi:https://doi.org/10.1016/j.eurpolymj.2018.10.042

Gharehkhani, S., Yarmand, H., Goodarzi, M. S., Shirazi, S. F. S., Amiri, A., Zubir, M. N. M., . . . Wongwises, S. (2017). Experimental investigation on rheological, momentum and heat transfer characteristics of flowing fiber crop suspensions. *International Communications in Heat and Mass Transfer, 80*, 60-69. doi:https://doi.org/10.1016/j.icheatmasstransfer.2016.11.013

Gong, W., Shen, J., Dai, W., Li, K., & Gong, M. (2021). Research and applications of drag reduction in thermal equipment: A review. *International Journal of Heat and Mass Transfer, 172*, 121152. doi:https://doi.org/10.1016/j.ijheatmasstransfer.2021.121152

Habibi, H., & Khosravi-Darani, K. (2017). Effective variables on production and structure of xanthan gum and its food applications: A review. *Biocatalysis and Agricultural Biotechnology, 10*, 130-140. doi:https://doi.org/10.1016/j.bcab.2017.02.013

Hasan, A. M. A., & Abdel-Raouf, M. E. (2018). Applications of guar gum and its derivatives in petroleum industry: A review. *Egyptian Journal of Petroleum, 27*(4), 1043-1050. doi:https://doi.org/10.1016/j.ejpe.2018.03.005

Hayder A. Abdul Bari, K. L. a. R. M. Y. (2011). Drag Reduction Characteristics Using Aloe Vera Natural Mucilage: An Experimental Study. *Journal of Applied Sciences*. doi:10.3923/jas.2011.1039.1043

Johnson, W. (2005). Final Report of the Safety Assessment of Acacia Catechu Gum, Acacia Concinna Fruit Extract, Acacia Dealbata Leaf Extract, Acacia Dealbata Leaf Wax, Acacia Decurrens Extract, Acacia Farnesiana Extract, Acacia Farnesiana Flower Wax, Acacia Farnesiana Gum, Acacia Senegal Extract, Acacia Senegal Gum, and Acacia Senegal Gum Extract. *International Journal of Toxicology - INT J TOXICOL, 24*, 75-118. doi:10.1080/10915810500257170

Khalid, S. A., Musa, A., Saeed, A., Elkhair Ali Ali, N., Abugroun, E. A., Mohamed, G., . . . Phillips, A. O. (2021). Gum Arabic in renal disease (GARDS Study): Clinical evidence of dietary supplementation impact on progression of renal dysfunction. *Journal of Functional Foods, 82*, 104515. doi:https://doi.org/10.1016/j.jff.2021.104515

Kumar, A., Rao, K. M., & Han, S. S. (2018). Application of xanthan gum as polysaccharide in tissue engineering: A review. *Carbohydrate Polymers, 180*, 128-144. doi:https://doi.org/10.1016/j.carbpol.2017.10.009

Lumley, J. L. (1969). Drag Reduction by Additives. *Annual Review of Fluid Mechanics, 1*(1), 367-384. doi:10.1146/annurev.fl.01.010169.002055

Maji, B., & Maiti, S. (2021). Chemical modification of xanthan gum through graft copolymerization: Tailored properties and potential applications in drug delivery and wastewater treatment. *Carbohydrate Polymers, 251*, 117095. doi:https://doi.org/10.1016/j.carbpol.2020.117095

Manzhai, V. N., Nasibullina, Y. R., Kuchevskaya, A. S., & Filimoshkin, A. G. (2014). Physico-chemical concept of drag reduction nature in dilute polymer solutions (the Toms effect). *Chemical Engineering and Processing, 80*, 38-42. doi:10.1016/j.cep.2014.04.003

Mate, C., & Mishra, S. (2020). Exploring the Potential of Moi Gum for Diverse Applications: A Review. *Journal of Polymers and the Environment, 28*. doi:10.1007/s10924-020-01709-8

Novelli, G. L., Ferrari, L. A., Vargas, G. G., & Loureiro, B. V. (2019). A synergistic analysis of drag reduction on binary polymer mixtures containing guar gum. *International Journal of Biological Macromolecules, 137*, 1121-1129. doi:https://doi.org/10.1016/j.ijbiomac.2019.07.042

Oprea, S., & Oprea, V. (2013). Synthesis and characterization of the cross-linked polyurethane–gum arabic blends obtained by multiacrylates cross-linking polymerization. *Journal of Elastomers and Plastics, 45*, 564-576. doi:10.1177/0095244312459281

Palaniraj, A., & Jayaraman, V. (2011). Production, recovery and applications of xanthan gum by Xanthomonas campestris. *Journal of Food Engineering, 106*(1), 1-12. doi:https://doi.org/10.1016/j.jfoodeng.2011.03.035

Saya, L., Malik, V., Singh, A., Singh, S., Gambhir, G., Singh, W. R., . . . Hooda, S. (2021). Guar gum based nanocomposites: Role in water purification through efficient removal of dyes and metal ions. *Carbohydrate Polymers, 261*, 117851. doi:https://doi.org/10.1016/j.carbpol.2021.117851

Sharma, G., Sharma, S., Kumar, A., Al-Muhtaseb, A. a. H., Naushad, M., Ghfar, A. A., . . . Stadler, F. J. (2018). Guar gum and its composites as potential materials for diverse applications: A review. *Carbohydrate Polymers, 199*, 534-545. doi:https://doi.org/10.1016/j.carbpol.2018.07.053

Soares, E. J., Siqueira, R. N., Leal, L. M., Barbosa, K. C. O., Cipriano, D. F., & Freitas, J. C. C. (2019). The role played by the aging of aloe vera on its drag reduction properties in turbulent flows. *Journal of Non-Newtonian Fluid Mechanics, 265*, 1-10. doi:https://doi.org/10.1016/j.jnnfm.2018.12.010

Sokhal, K., Dasaroju, G., & Bulasara, V. (2019). Effect-of-Reynolds-number-and-concentration-of-biopolymer-gum-arabic-on-drag-reduction-of-turbulent-flow-in-circular-pipe.

Tamano, S., Ikarashi, H., Morinishi, Y., & Taga, K. (2015). Drag reduction and degradation of nonionic surfactant solutions with organic acid in turbulent pipe flow. *Journal of Non-Newtonian Fluid Mechanics, 215*, 1-7. doi:https://doi.org/10.1016/j.jnnfm.2014.10.011

Tiong, A. N. T., Kumar, P., & Saptoro, A. (2015). Reviews on drag reducing polymers. *Korean Journal of Chemical Engineering, 32*(8), 1455-1476. doi:10.1007/s11814-015-0104-0

Verma, C., & Quraishi, M. A. (2021). Gum Arabic as an environmentally sustainable polymeric anticorrosive material: Recent progresses and future opportunities. *International Journal of Biological Macromolecules*. doi:https://doi.org/10.1016/j.ijbiomac.2021.06.050

Verma, D., & Sharma, S. K. (2021). Recent advances in guar gum based drug delivery systems and their administrative routes. *International Journal of Biological Macromolecules, 181*, 653-671. doi:https://doi.org/10.1016/j.ijbiomac.2021.03.087

Yu, C., Liu, M., Zhang, C., Yan, H., Zhang, M., Wu, Q., . . . Jiang, L. (2020). Bio-inspired drag reduction: From nature organisms to artificial functional surfaces. *Giant, 2*, 100017. doi:https://doi.org/10.1016/j.giant.2020.100017

Zhang, Y., Zhou, F., & Kang, J. (2020). Flow and heat transfer in drag-reducing polymer solution flow through the corrugated tube and circular tube. *Applied Thermal Engineering, 174*, 115185. doi:https://doi.org/10.1016/j.applthermaleng.2020.115185